tanoylation modification at Ser^3 [18, 19]. This peptide stimulates gastric motility and accelerates postprandial gastric emptying in human volunteers [20]. Acceleration of gastric emptying by ghrelin has also been observed in patients with diabetic, idiopathic, and post vagotomy gastroparesis, although the numbers of patients enrolled in those studies were small [21-23]. In addition, ghrelin stimulates food intake following peripheral administration [24, 25]. Therefore, we hypothesized that ghrelin might be useful for the treatment of GI disorders related to SSc.

In this study, we investigated whether administration of ghrelin could improve gastric emptying in outpatients with GI symptoms due to SSc. We also evaluated the safety of ghrelin injection to treat GI involvement in patients with SSc.

Subjects and Methods

Patients

To be included in this study, subjects had to have SSc as defined by the American College of Rheumatology (ACR) (Table 1) and exhibit GI involvement. Criteria for GI involvement included gastroesophageal reflux disease (GERD), dysphasia, early satiety, postprandial fullness, bloating, bacterial overgrowth requiring antibiotics, abdominal pain, diarrhea, and/or malabsorption syndrome (Table 2). Exclusion criteria were 1) localized scleroderma; 2) esophageal stenosis; 3) receiving parenteral or enteral nutrition; 4) past history of open-abdominal surgery of the GI tract; 5) allergy against milk or liquid meal (Racol^{TM}); 6) severe hepato-renal or respiratory disorders, severe depression, schizophrenia, mania, severe diabetes, congenital amino-acid metabolic disorder; 7) tendency or past history of suicide; 8) pregnancy; 9) lactation; and 10) past history of malignant tumors. Medication that had already been started before the initial enrolment could be continued during this study. During the entire period of this study, any additional drugs that might influence the study outcome, including prokinetics, antipeptic ulcer agents, and drugs to treat intestine, liver, gallbladder, or pancreatic disease, were not allowed at any time. The initial planned sample size was ten or more. Patient registration lasted from Oct 2010 to Aug 2011. The study protocol was approved by the Ethics Committees on Human Research of the Kyoto University Graduate School of Medicine. We obtained written informed consent from all subjects prior to enrolment. This study was conducted according to the Declaration of Helsinki principals. This trial was registered at the UMIN Clinical Trials Registry as UMIN000003739.

Table 1 Criteria for the Classification of Systemic Sclerosis (Defined by the American College of Rheumatology [ACR])

Major criterion:
• Proximal diffuse (truncal) sclerosis (skin tightness, thickening, non-pitting induration)
Minor criteria:
• Sclerodactyly (only fingers and/or toes)
• Digital pitting scars or loss of substance of the digital finger pads (pulp loss)
• Bilateral basilar pulmonary fibrosis
The patient should fulfill the major criterion or two of the three minor criteria.

Table 2 Grading of Gastrointestinal Involvement in Systemic Sclerosis (Draft Guidelines of Japan)

Upper Digestive Tract
1. Normal
2. Mild: No symptom, but with decreased peristalsis in the lower esophagus
3. Moderate: Gastroesophageal Reflux Disease (GERD)
4. Severe: Dysphagia caused by reflux esophagitis
5. Very Severe: Dysphagia caused by esophageal stenosis
Lower Digestive Tract
1. Normal
2. Mild: Intestinal lesions such as bloating, abdominal pain, diarrhea, etc. with no need for antibiotics
3. Moderate: Overgrowth of enteric bacteria with need for antibiotics
4. Severe: Chronic intestinal pseudo-obstruction or malabsorption syndrome
5. Very Severe: Received intravenous hyperalimentation

Study design

The study was performed in a randomized, double-blind, placebo-controlled two-period crossover fashion on two occasions with a washout interval of at least 2 weeks (Fig. 1). Medication that might affect gastric motility (e.g.: metoclopramide, anticholinergics, calcium channel antagonists, macrolide antibiotics) was discontinued at least 24 hours before ^{13}C-acetic acid breath test. After a 12-hour fast, SSc patients underwent ^{13}C-acetic acid breath test; breath testing started between 8:30 and 9:00 am. Liquid meal (Racol^{TM}, Otsuka Pharmaceutical Co., Ltd., Tokyo, Japan) was used as the test meal. The nutrient composition of 100 mL of liquid meal (100 kcal) is 4.4 g of protein, 15.6 g of carbohydrate, and 2.2 g of fat. ^{13}C was used to label

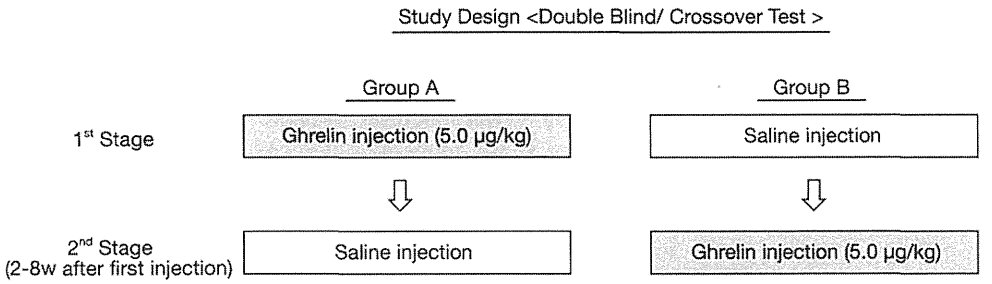

Fig. 1 Schematic of the study schedule.
Ghrelin (5.0 μg/kg) and placebo were administered in a randomized, double-blind, placebo-controlled, and cross-over fashion on 2 separate days at least 2 weeks apart.

acetate (99%; Cambridge Isotope Laboratories, Woburn, MA, USA), which is absorbed in the duodenum but not in the stomach. Liquid meal was mixed with ^{13}C-acetate (100 mg), and all patients ingested 200 mL of test meal within a few minutes. Ghrelin (5.0 μg/kg) or placebo was injected intravenously over 30 seconds immediately after ingestion of the test meal. Breath samples were collected for $^{13}CO_2$ measurement before the meal, and then every 15 minutes for 3.5 hours. During each expiration phase, exhaled air was collected into a bag a total of 15 times. The concentration of $^{13}CO_2$ was measured using a gas chromatograph isotope-ratio mass spectrometer (UBiT-IR300, Ootsuka Electronic Corp), and the measured values were presented as the delta-$^{13}CO_2$ (expressed as a percentage). To evaluate the effect of ghrelin on gastric emptying, T_{max} was defined as the time taken to reach the maximum concentration, calculated using the delta-$^{13}CO_2$ values.

T_{max} assessed by ^{13}C-acetate breath test

The ^{13}C-acetate breath test was developed as a non-radioactive alternative for the measurement of gastric emptying. Braden and colleagues [26] reported that half-emptying times for the ^{13}C-acetate breath test were closely correlated with those measured by radioscintigraphy, using both semisolids and liquids, and that the T_{max} of $^{13}CO_2$ exhalation was itself a reliable parameter compared with the half-emptying times obtained by scintigraphy.

Primary endpoint

The primary endpoint of this trial was T_{max} assessed by ^{13}C-acetic acid breath test.

Secondary endpoint

The secondary endpoints of this trial were alteration in hunger sensation and serum GH levels upon ghrelin or placebo administration.

Assessment of satiety

Visual analogue scale (VAS) scores, 10 cm in length, were used to assess satiety [27-29]. VASs were completed pre-infusion and 15, 30, 60, and 90 min after ghrelin or saline administration. The positions on the scale were measured in centimeters.

Measurement of serum GH concentration

Blood samples for measurement of GH were drawn before ingestion of the test meal and 30 minutes after ghrelin or saline infusion. Serum GH concentrations (normal values: male, <1.46; female, 0.28–8.70 ng/mL) were measured by IRMA (Mitsubishi Kagaku Bio-Clinical Laboratories Inc., Tokyo, Japan).

Measurement of plasma ghrelin levels

Measurement of plasma ghrelin levels was performed as reported previously [30]. Blood samples drawn from a forearm vein were immediately transferred to chilled siliconized glass tubes containing Na_2EDTA (1 mg/mL) and aprotinin (1000 KIU/mL, Ohkura Pharmaceutical, Kyoto, Japan). After centrifugation at 4°C to separate out the plasma, hydrochloric acid was added to samples at a final concentration of 0.1 N. Plasma was immediately frozen and stored at −80°C prior to the assay. Plasma ghrelin concentrations were determined using a ghrelin ELISA kit (Mitsubishi Kagaku Iatron, Tokyo, Japan).

Assessment of safety

Vital signs, including blood pressure, pulse rate, and body temperature, were measured during examination. Changes in physical symptoms were assessed by phone interview 2 weeks after ghrelin or saline injection. If the study was interrupted, assessments of safety by

hematology, blood chemistry, and urine analysis were performed when the study was discontinued.

Ghrelin

Human ghrelin was prepared as described previously [28]. Ghrelin was dissolved in 3.75% D-mannitol to a final concentration of 180 μg/mL. Solutions were filtered and stored at −20°C in sterile vials. Examination by the Japan Food Research Laboratories (Tokyo, Japan) did not find any traces of endotoxin in the ghrelin solutions; a pyrogen test based on the Pharmacopoeia of Japan was also negative.

Statistical evaluations

A sample size of 10 patients was required to provide at least 90% power to detect a T_{max} ratio of 0.70 between treatments with a standard deviation of 30 minutes and an intra-patient correlation coefficient of 0.50 or more. This ratio was based on data from previous studies. All statistical analysis of the two-period cross-over design was performed using a linear mixed-effect model with treatment period as fixed effects and patient as the random effect. The 95% confidence intervals (CIs) for group means and treatment differences were estimated using least-squares means (LS-means) and robust variance. Carry-over effects were assessed using the test for the treatment by period interaction term in linear mixed-effect models. All statistical analyses were performed using the SAS software, version 8 (SAS Institute Inc., Cary, NC, USA). A two-tailed *P*-value was used, with the required level of significance set at 0.05.

Results

Baseline characteristics of subjects

Ten subjects (seven women, median age 67.5 years, range 48–80 years) were enrolled in this study (Table 3). All ten subjects were diagnosed with SSc, as defined by the criteria of the American College of Rheumatology (ACR); all subjects fulfilled the major criterion. Three subjects had diffuse SSc, and seven had limited SSc. Anti–topoisomerase I antibodies were positive in two patients, and anti-centromere antibodies were positive in four patients. As shown in Table 3, all subjects exhibited GI involvement; nine had early satiety and postprandial fullness, seven had heart burn and dysphagia caused by reflux esophagitis, and two had diarrhea. Average BMI at registration was 21.1 ± 4.2 kg/m^2. None took H_2-blockers or antibiotics. One patient (Patient No. 2) discontinued this examination after the first injection (saline) because of a gallbladder stone attack.

Clinical effects

Plasma levels of ghrelin 30 minutes were 999.2 ± 23.7 fmol/mL after ghrelin injection (pre-injection, 20.2 ± 10.3 fmol/mL) and 15.4 ± 6.0 fmol/mL after saline injection (pre-injection, 18.8 ± 7.4 fmol/mL). As shown in Fig. 2, serum GH levels were significantly elevated after ghrelin administration (ghrelin *vs.* saline: 61.9 ± 9.5 *vs.* 1.4 ± 1.2 ng/mL).

Ghrelin shortened gastric emptying time in patients with SSc (Fig. 3). Gastric emptying, as determined evaluated by ^{13}C-acetic acid breath test, was signifi-

Table 3 Baseline characteristics

Patient No.	Sex	Age	BMI	subtypes	AT1A	ACA	Gastrointestinal Symptoms			Gastrointestinal Drugs	
							Postprandial Fullness	Dysphagia	Diarrhea	Prokinetics	PPI
1	M	68	26.3	diffuse	-	-	+	-	-	-	-
2	M	48	21.2	diffuse	+	-	+	-	+	+	+
4	F	57	22.2	limited	-	+	+	+	-	+	+
5	F	71	17.4	limited	-	+	+	+	-	+	+
6	M	76	20.2	limited	-	-	+	+	-	-	+
7	F	62	18.8	limited	-	-	-	+	-	-	+
8	F	73	17.7	limited	-	+	+	+	-	+	+
9	F	66	30.1	limited	-	+	+	+	-	+	+
11	F	80	18.1	diffuse	+	-	+	+	+	+	+
12	F	50	18.8	limited	-	-	+	-	-	+	+

ACA, anti-centromere antibody; AT1A, anti–topoisomerase 1 antibody

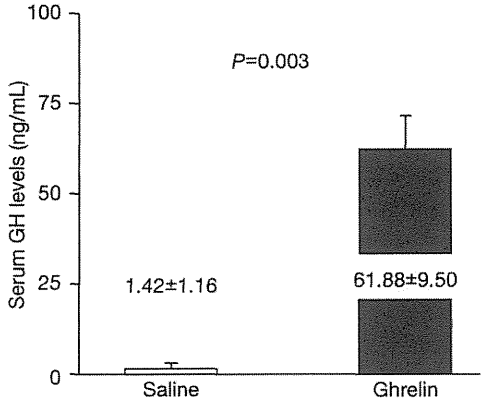

Fig. 2 Serum growth hormone levels 30 minutes after ghrelin or saline injection
Data are shown as means ± SD (n=9).

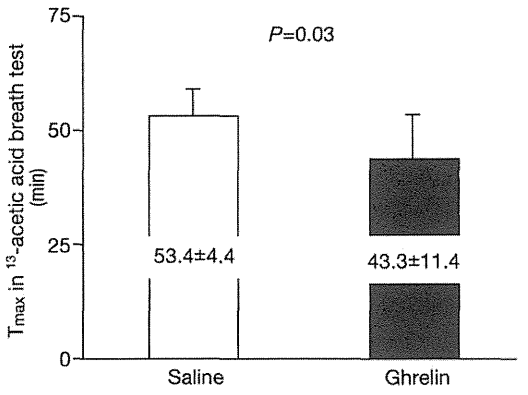

Fig. 3 Gastric emptying of the liquid test meal
Gastric emptying was evaluated by ^{13}C-acetic acid breath test. T_{max} was defined as the time taken to reach the maximum concentration. Data are shown as means ± SD (n=9).

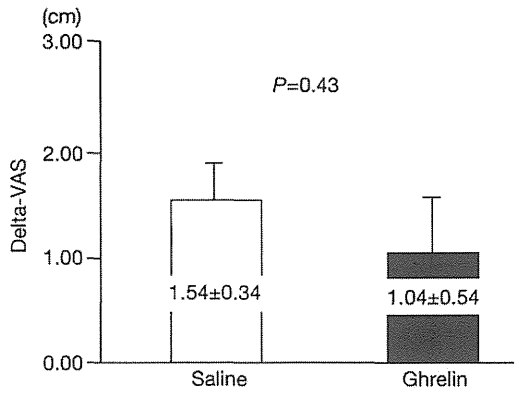

Fig. 4 Effect of ghrelin on appetite in patients with SSc.
The data are shown as changes in the visual analog scores (VAS) after ghrelin or saline injection: maximum value after injection minus value prior to injection (means ± SD; n=9).

cantly accelerated by ghrelin injection (43.3 min, 95% CI 31.8–54.7 min) relative to saline injection (53.4 min, 95% CI 47.4–59.3 min; treatment difference −10.1 min, 95% CI −19.1–−1.2 min, P=0.03). There was no carry-over effect in the primary endpoint (P=0.17 by interaction test). The effects of ghrelin on appetite were assessed by changes in the visual analog scores (VAS) before and after ghrelin or placebo injection. Delta-VAS was calculated as the maximum value after administration minus the value before administration. Thus, the larger amounts of changes in VAS indicated an improvement in early satiety after ghrelin or saline injection. As shown in Fig. 4, however, administration with ghrelin did not improve early satiety. No significant carryover effect or interaction effect was observed (P=0.06).

Adverse effects

No serious adverse effects were observed. We observed two moderate events, flushing and sweating, with incidences similar to those previously reported. These complaints were transient and well tolerated.

Discussion

Administration of ghrelin induces the migrating motor complex in fasting rat and human and accelerates postprandial gastric motility in healthy humans and patients with idiopathic, neurogenic, or diabetic gastroparesis [21-24]. In previous studies, $T_{1/2\ liq}$ (half-emptying time for liquids, in minutes) decreased by 20–30% following injection of 0.7–5.9 μg/kg of ghrelin. We previously reported that ghrelin tended to increase appetite in a dose-dependent manner (i.e., more so at 5.0 than 1.0 μg/kg) in a phase I study, and that it is safe at a dose of 5.0 μg/kg [27, 28, 31]. Based on these findings, we adopted the present protocol.

This study is the first clinical investigation to demonstrate that a single administration of ghrelin significantly accelerated gastric emptying time, relative to placebo, in patients with SSc who had current symptoms suggestive of gastroparesis; the improvement rate was about 23%. This observation is in line with animal studies and with previous reports of a stimulatory effect of a similar dose of ghrelin on gastric motility in humans [20-25]. We initially expected that administration of ghrelin would improve GI motility, result in relief of GI symptoms. However, although the gastric emptying rate was increased following ghrelin

administration, post-prandial satiety did not improved. Franck-Larsson *et al.* reported that delayed gastric emptying in SSc did not relate to gastrointestinal symptoms or myoelectric gastric activity [5]. Taken together, these observations suggest that factors other than gastric motility might contribute to upper gastrointestinal symptoms.

Several prokinetic agents, such as metoclopramide, domperidone, erythromycin, mosapride citrate, and dinoprost, have been used in attempts to improve GI motility in patients with SSc who suffered from gastroparesis; however, therapies with these agents are usually unsatisfactory [13-17]. Soudah *et al.* had reported that octreotide stimulates intestinal motility and reduces bacterial overgrowth, resulting in improvement in abdominal symptoms [15]. Based on that report, we predict that octreotide could be adapted to the treatment of gastric involvement in patients with SSc. Like octreotide, ghrelin may also have therapeutic potential for the treatment of GI dismotility in patients with SSc. Because this study was designed with a single-dose and single-injection protocol, larger-scale and longer-term prospective cohort studies are needed to define the effects of ghrelin on gastric motility in patients with SSc. Also, future studies should investigate whether ghrelin treatment can improve gastrointestinal symptoms.

Cohen *et al.* proposed a two-stage process in the pathophysiology of SSc: a neuropathic phase followed by a myopathic phase [32]. The second phase is characterized by smooth-muscle atrophy and replacement of muscle tissue with fibrosis. From that perspective, it is likely that ghrelin would not be effective for the treatment of SSc patients with second-phase gastroparesis. Although experiments in chemically or surgically vagotomized animals have suggested that the motility effects of ghrelin are caused mainly by activation of vagal afferents [33, 34], the ghrelin receptor is expressed in the enteric nerve system [35, 36]; furthermore, *in vitro*, ghrelin increases electrically induced contraction of rat and mouse muscle strips [37-40]. In addition, in previous studies, injection of ghrelin accelerated gastric motility in patients with neurogenic and diabetic gastroparesis [21-24]. Thus, we expect that ghrelin, at least, is effective for the treatment of SSc patients with first-phase gastroparesis.

There are some limitations in the present study such as small sample size, single dose and single attempt for ghrelin infusion. However, the results of this study suggest that ghrelin may have therapeutic potential for the treatment of GI dismotility in patients with SSc. Further studies using more subjects and with multiple injections of ghrelin will be required in order to confirm the effects of ghrelin on gastric motility and gastrointestinal symptoms in patients with SSc.

Acknowledgements

This study was supported by funds from the Ministry of Education, Science, Culture, Sports and Technology of Japan; the Ministry of Health, Labour and Welfare of Japan; the Tokyo Biochemical Research Foundation; and the Foundation for Growth Science. We would like to thank K. Amemiya for her excellent secretarial assistance, and C. Ishimoto and C. Shiraiwa for their excellent technical assistance. We would also like to thank H. Endo at Toho University for his special technical advice.

Conflict of Interest

The authors have no conflict of interest and nothing to disclose.

References

1. Sjogren RW (1994) Gastrointestinal motility disorders in scleroderma. *Arthritis Rheum* 37: 1265-1282.
2. Forbes A, Marie I (2009) Gastrointestinal complications: the most frequent internal complications of systemic sclerosis. *Rheumatology (Oxford)* 48 Suppl 3: iii36-39.
3. D'Angelo WA, Fries JF, Masi AT, Shulman LE (1969) Pathologic observations in systemic sclerosis (scleroderma). A study of fifty-eight autopsy cases and fifty-eight matched controls. *Am J Med* 46: 428-440.
4. Bortolotti M, Turba E, Tosti A, Sarti P, Brunelli F, et al. (1991) Gastric emptying and interdigestive antroduodenal motility in patients with esophageal scleroderma. *Am J Gastroenterol* 86: 743-747.
5. Franck-Larsson K, Hedenstrom H, Dahl R, Ronnblom A (2003) Delayed gastric emptying in patients with diffuse versus limited systemic sclerosis, unrelated to gastrointestinal symptoms and myoelectric gastric activity.

Scand J Rheumatol 32: 348-355.
6. Maddern GJ, Horowitz M, Jamieson GG, Chatterton BE, Collins PJ, et al. (1984) Abnormalities of esophageal and gastric emptying in progressive systemic sclerosis. *Gastroenterology* 87: 922-926.
7. Marycz T, Muehldorfer SM, Katalinic A, Herold C, Ell C, et al. (1999) Gastric involvement in progressive systemic sclerosis: electrogastrographic and sonographic findings. *Eur J Gastroenterol Hepatol* 11: 1151-1156.
8. Mittal BR, Wanchu A, Das BK, Ghosh PP, Sewatkar AB, et al. (1996) Pattern of gastric emptying in patients with systemic sclerosis. *Clin Nucl Med* 21: 379-382.
9. Sridhar KR, Lange RC, Magyar L, Soykan I, McCallum RW. (1998) Prevalence of impaired gastric emptying of solids in systemic sclerosis: diagnostic and therapeutic implications. *J Lab Clin Med* 132: 541-546.
10. Wedmann B, Wegener M, Adamek RJ, el Gammal S (1994) Gastrobiliary motility after liquid fatty meal in progressive systemic sclerosis: a sonographic study. *Dig Dis Sci* 39: 565-570.
11. Wegener M, Adamek RJ, Wedmann B, Wedmann B, Jergas M, et al. (1994) Gastrointestinal transit through esophagus, stomach, small and large intestine in patients with progressive systemic sclerosis. *Dig Dis Sci* 39: 2209-2215.
12. Marie I, Gourcerol G, Leroi AM, Ménard JF, Levesque H, et al. (2012) Delayed gastric emptying determined using the 13C-octanoic acid breath test in patients with systemic sclerosis. *Arthritis Rheum* 64: 2346-2355.
13. Johnson DA, Drane WE, Curran J, Benjamin SB, Chobanian SJ, et al. (1987) Metoclopramide response in patients with progressive systemic sclerosis. Effect on esophageal and gastric motility abnormalities. *Arch Intern Med* 147: 1597-1601.
14. Smout AJ, Bogaard JW, Grade AC, ten Thije OJ, Akkermans LM, et al. (1985) Effects of cisapride, a new gastrointestinal prokinetic substance, on interdigestive and postprandial motor activity of the distal oesophagus in man. *Gut* 26: 246-251.
15. Soudah HC, Hasler WL, Owyang C. (1991) Effect of octreotide on intestinal motility and bacterial overgrowth in scleroderma. *N Engl J Med* 325: 1461-1467.
16. Dull JS, Raufman JP, Zakai MD, Strashun A, Straus EW (1990) Successful treatment of gastroparesis with erythromycin in a patient with progressive systemic sclerosis. *Am J Med* 89: 528-530.
17. Tomomasa T, Kuroume T, Arai H, Wakabayashi K, Itoh Z (1986) Erythromycin induces migrating motor complex in human gastrointestinal tract. *Dig Dis Sci* 31: 157-161.
18. Kojima M, Hosoda H, Date Y, Nakazato M, Matsuo H, et al. (1999) Ghrelin is a growth-hormone-releasing acylated peptide from stomach. *Nature* 402: 656-660.
19. Ariyasu H, Takaya K, Tagami T, Ogawa Y, Hosoda K, et al. (2001) Stomach is a major source of circulating ghrelin, and feeding state determines plasma ghrelin-like immunoreactivity levels in humans. *J Clin Endocrinol Metab* 86: 4753-4758.
20. Levin F, Edholm T, Schmidt PT, Grybäck P, Jacobsson H, et al. (2006) Ghrelin stimulates gastric emptying and hunger in normal-weight humans. *J Clin Endocrinol Metab* 91: 3296-3302.
21. Murray CD, Martin NM, Patterson M, Taylor SA, Ghatei MA, et al. (2005) Ghrelin enhances gastric emptying in diabetic gastroparesis: a double blind, placebo controlled, crossover study. *Gut* 54: 1693-1698.
22. Tack J, Depoortere I, Bisschops R, Verbeke K, Janssens J, et al. (2005) Influence of ghrelin on gastric emptying and meal-related symptoms in idiopathic gastroparesis. *Aliment Pharmacol Ther* 22: 847-853.
23. Binn M, Albert C, Gougeon A, Maerki H, Coulie B, et al. (2006) Ghrelin gastrokinetic action in patients with neurogenic gastroparesis. *Peptides* 27: 1603-1606.
24. Shin A, Camilleri M, Busciglio I, Burton D, Stoner E, et al. (2013) Randomized controlled phase Ib study of ghrelin agonist, RM-131, in type 2 diabetic women with delayed gastric emptying: pharmacokinetics and pharmacodynamics. *Diabetes Care* 36: 41-48.
25. Wren AM, Seal LJ, Cohen MA, Brynes AE, Frost GS, et al. (2001) Ghrelin enhances appetite and increases food intake in humans. *J Clin Endocrinol Metab* 86: 5992-5995.
26. Braden B, Adamas S, Duan L, Orth KH, Maul FD, et al. (1995) The ^{13}C acetate breath test accurately reflects gastric emptying of liquids in both liquids and semisolid test meals. *Gastroenterology* 108: 1048-1055.
27. Akamizu T, Iwakura H, Ariyasu H, Hosoda H, Murayama T, et al. (2008) Repeated administration of ghrelin to patients with functional dyspepsia: its effects on food intake and appetite. *Eur J Endocrinol* 158: 491-498.
28. Akamizu T, Takaya K, Irako T, Hosoda H, Teramukai S, et al. (2004) Pharmacokinetics, safety, and endocrine and appetite effects of ghrelin administration in young healthy subjects. *Eur J Endocrinol* 150: 447-455.
29. Thompson DA, Campbell RG (1977) Hunger in humans induced by 2-deoxy-D-glucose: glucoprivic control of taste preference and food intake. *Science* 198: 1065-1068.
30. Ariyasu H, Iwakura H, Yamada G, Kanamoto N, Bando M, et al. (2010) A postweaning reduction in circulating ghrelin temporarily alters growth hormone (GH) responsiveness to GH-releasing hormone in male mice but does not affect somatic growth. *Endocrinology* 151: 1743-5170.
31. Akamizu T, Iwakura H, Ariyasu H, Murayama T, Sumi E, et al. (2008) Effects of ghrelin treatment on patients undergoing total hip replacement for osteoarthritis: different outcomes from studies in patients with cardiac and pulmonary cachexia. *J Am Geriatr Soc* 56: 2363-

2365.
32. Cohen S, Fisher R, Lipshutz W, Turner R, Myers A, et al. (1972) The pathogenesis of esophageal dysfunction in scleroderma and Raynaud's disease. *J Clin Invest* 51: 2663-2668.
33. Fujino K, Inui A, Asakawa A, Kihara N, Fujimura M, et al. (2003) Ghrelin induces fasted motor activity of the gastrointestinal tract in conscious fed rats. *J Physiol* 550: 227-240.
34. Edholm T, Levin F, Hellström PM, Schmidt PT (2004) Ghrelin stimulates motility in the small intestine of rats through intrinsic cholinergic neurons. *Regul Pept* 121: 25-30.
35. Xu L, Depoortere I, Tomasetto C, Zandecki M, Tang M, et al. (2005) Evidence for the presence of motilin, ghrelin, and the motilin and ghrelin receptor in neurons of the myenteric plexus. *Regul Pept* 124: 119-125.
36. Dass NB, Munonyara M, Bassil AK, Hervieu GJ, Osbourne S, et al. (2003) Growth hormone secretagogue receptors in rat and human gastrointestinal tract and the effects of ghrelin. *Neuroscience* 120: 443-453.
37. Fukuda H, Mizuta Y, Isomoto H, Takeshima F, Ohnita K, et al. (2004) Ghrelin enhances gastric motility through direct stimulation of intrinsic neural pathways and capsaicin-sensitive afferent neurones in rats. *Scand J Gastroenterol* 39: 1209-1214.
38. Bassil AK, Dass NB, Sanger GJ (2006) The prokinetic-like activity of ghrelin in rat isolated stomach is mediated via cholinergic and tachykininergic motor neurons. *Eur J Pharmacol* 544: 146-152.
39. Kitazawa T, De Smet B, Verbeke K, Depoortere I, Peeters TL (2005) Gastric motor effects of peptide and non-peptide ghrelin agonists in mice in vivo and in vitro. *Gut* 54: 1078-1084.
40. Depoortere I, De Winter B, Thijs T, De Man J, Pelckmans P, et al. (2005) Comparison of the gastroprokinetic effects of ghrelin, GHRP-6 and motilin in rats in vivo and in vitro. *Eur J Pharmacol* 515: 160-168.

THE JOURNAL OF BIOLOGICAL CHEMISTRY VOL. 289, NO. 3, pp. 1564–1579, January 17, 2014

Functional Evaluation of Activation-dependent Alterations in the Sialoglycan Composition of T Cells*

Received for publication, October 6, 2013, and in revised form, November 28, 2013 Published, JBC Papers in Press, December 2, 2013, DOI 10.1074/jbc.M113.523753

Yuko Naito-Matsui[‡], Shuhei Takada[‡], Yoshinobu Kano[‡], Tomonori Iyoda[§], Manabu Sugai[¶], Akira Shimizu[¶], Kayo Inaba[§], Lars Nitschke[‖], Takeshi Tsubata[**], Shogo Oka[‡‡], Yasunori Kozutsumi[‡], and Hiromu Takematsu[‡ ‡‡1]

From the [‡]Laboratory of Membrane Biochemistry and Biophysics and the [§]Laboratory of Immunology, Graduate School of Biostudies, Kyoto University, 46-29 Yoshida-shimoadachi, Sakyo, Kyoto 606-8501, Japan, the [¶]Department of Experimental Therapeutics, Translational Research Center, Kyoto University Hospital, 54 Shogoin-Kawahara, Sakyo, Kyoto 606-8507, Japan, the [‖]Department of Biology, University of Erlangen, 91058 Erlangen, Germany, the [**]Department of Immunology, Medical Research Institute, Tokyo Medical and Dental University, 1-5-45 Yushima, Bunkyo-ku, Tokyo 113-8510, Japan, and the [‡‡]Department of Biological Chemistry, Human Health Sciences, Graduate School of Medicine, Kyoto University, 53 Shogoin-Kawahara, Sakyo, Kyoto 606-8507, Japan

Background: Sialic acids play key roles in molecular recognition.
Results: T-cell activation alters the principal sialic acid species profile, regulating expression of siglec ligands, T-cell activation *per se*, and T cell-B cell interactions.
Conclusion: This activation-dependent change in the sialoglycan profile modulates immune responses.
Significance: Pronounced changes in the sialoglycan profile not only serve as cellular markers but also reflect cellular functionality.

Sialic acids (Sias) are often conjugated to the termini of cellular glycans and are key mediators of cellular recognition. Sias are nine-carbon acidic sugars, and, in vertebrates, the major species are *N*-acetylneuraminic acid (Neu5Ac) and *N*-glycolylneuraminic acid (Neu5Gc), differing in structure at the C5 position. Previously, we described a positive feedback loop involving regulation of Neu5Gc expression in mouse B cells. In this context, Neu5Gc negatively regulated B-cell proliferation, and Neu5Gc expression was suppressed upon activation. Similarly, resting mouse T cells expressed principally Neu5Gc, and Neu5Ac was induced upon activation. In the present work, we used various probes to examine sialoglycan expression by activated T cells in terms of the Sia species expressed and the linkages of Sias to glycans. Upon T-cell activation, sialoglycan expression shifted from Neu5Gc to Neu5Ac, and the linkage shifted from α2,6 to α2,3. These changes altered the expression levels of sialic acid-binding immunoglobulin-like lectin (siglec) ligands. Expression of sialoadhesin and Siglec-F ligands increased, and that of CD22 ligands decreased. Neu5Gc exerted a negative effect on T-cell activation, both in terms of the proliferative response and in the context of activation marker expression. Suppression of Neu5Gc expression in mouse T and B cells prevented the development of nonspecific CD22-mediated T cell-B cell interactions. Our results suggest that an activation-dependent shift from Neu5Gc to Neu5Ac and replacement of α2,6 by α2,3 linkages may regulate immune cell interactions at several levels.

When naive T cells encounter specific antigens, such cells differentiate into effector T cells and evoke immune responses via secretion of cytokines or the killing of infected cells. Therefore, control of T-cell activation is important to optimize the immune response. Upon activation, T cells undergo a variety of changes in glycosylation patterns (1–7), but the functional roles of such changes remain unclear (8). It is necessary to understand activation-dependent changes in glycosylation not only to define the mechanism of T cell-mediated immune regulation but also to support efforts to artificially modulate immune responses because glycans are located in the outermost regions of cells and are highly accessible.

T-cell activation is induced by recognition by T-cell receptors (TCRs)[2] of certain antigens displayed on the surfaces of antigen-presenting cells. TCR signaling is regulated by nearby co-receptors, allowing the same TCR to transmit signals from a single antigen triggering both apoptosis and activation. Glycosylation patterns are cell type-specific and change upon activation (6). Thus, many glycan-specific probes have been used as markers to define cell subpopulations or activated cells (9–12), although the functions of such markers remain unclear. Most membrane proteins, including the co-receptors and other signaling molecules, are glycoproteins, and changes in glycosylation patterns regulate function either by altering protein binding to glycan-binding proteins or lectins or by directly modulating protein activity (13). Collectively, co-receptor

* This work was supported by grants-in-aid from the Ministry of Education, Culture, Sports, Science and Technology of Japan; the Uehara Memorial Foundation; the Suzuken Memorial Foundation; and CREST, Japan Science and Technology Agency.
[1] To whom correspondence should be addressed: Human Health Sciences, Graduate School of Medicine, Kyoto University, 53 Shogoin-Kawahara, Sakyo, Kyoto 606-8507, Japan. Tel.: 81-75-751-3954; E-mail: htakema@pharm.kyoto-u.ac.jp.

[2] The abbreviations used are: TCR, T-cell receptor; BCR, B cell receptor; CMAH, CMP-Neu5Ac hydroxylase; CTL, cytotoxic T lymphocyte; GC, germinal center; IRES, internal ribosomal entry site; Neu5Ac, *N*-acetylneuraminic acid; Neu5Gc, *N*-glycolylneuraminic acid; Sia, sialic acid; siglec, sialic acid-binding immunoglobulin-like lectin; ConA, concanavalin A; Tg, transgenic; PE, phycoerythrin; IS, internal standard; CFSE, 5-(and-6)-carboxyfluorescein diacetate, succinimidyl ester; mSn, mouse sialoadhesin; DC, dendritic cell; T-B interaction, T cell-B cell interaction.

activities may be finely tuned by regulating glycosylation in a manner reflecting cellular status.

Study of glycosylation changes during T-cell activation has been an active field of glycobiology (6). The peanut lectin, PNA, binds to the desialylated core 1 of *O*-linked glycans, and expression of this epitope is developmentally regulated via sialylation-dependent masking. Thus, induction of PNA epitope expression on activated T cells is triggered by suppression of the activity of the sialyltransferase ST3GalI (7, 14), and the PNA epitope occurs on glycoproteins such as CD43 and CD45 (6). Expression of the core 2 branches of *O*-glycans is also regulated during T-cell activation. Levels of C2GnT increase, and the branching pattern changes in a manner that allows subsequent polylactosamine-mediated extension (15). After fucosylation enzyme(s) acts, such changes may regulate sialyl-Lewis^X expression, triggering homing of a subset of T cells via selectin-mediated cell adhesion (16). Overall, the surface glycans of T cells change upon activation, reflecting cell functionality (17).

The sialic acids (Sias) (18) form a family of nine-carbon acidic sugars that are often conjugated to glycan termini via α2,3-, 2,6-, and 2,8-linkages. Of the diverse Sia family members with various molecular modifications, *N*-acetylneuraminic acid (Neu5Ac) and *N*-glycolylneuraminic acid (Neu5Gc) are the major Sia species in mammals and differ by the presence of a hydroxy group at the C5 position (19). Resting B and T cells express Neu5Gc abundantly; however, we previously showed that the major Sia species changed from Neu5Gc to Neu5Ac upon activation of B cells, including germinal center (GC) B cells (4). Such suppression of Neu5Gc expression upon activation is achieved via repression of CMP-Neu5Ac hydroxylase (CMAH), an enzyme required for Neu5Gc biosynthesis from Neu5Ac at the sugar-nucleotide level (20, 21). Previously, we also found that a GL7 monoclonal antibody, a widely used GC marker, recognized α2,6-linked Neu5Ac and could be used to detect activation-dependent repression of Neu5Gc expression in B cells in which activation was negatively regulated by Neu5Gc. Resting T cells became GL7-positive upon stimulation with concanavalin A (ConA) (11). The major Sia species in resting T cells, as in B cells, is Neu5Gc. Thus, we hypothesized that the major Sia species of T cells would change from Neu5Gc to Neu5Ac upon activation. Indeed, Redelinghuys *et al.* (22) recently reported that levels of Neu5Gc and *Cmah* mRNA decreased in T cells upon *in vitro* activation. Furthermore, Yusuf *et al.* (23) found that follicular helper T cells (T_{FH} cells) within GCs could be distinguished from non-GC T_{FH} cells and that GC T_{FH} cells were GL7-positive, indicating that GC T_{FH} cells expressed Neu5Ac abundantly. GL7-positive GC T_{FH} cells mediate certain activities of GCs that are crucial steps in the development of the T cell-dependent immune response (24, 25). However, the functional significance of the change in the predominant Sia species of T cells requires further study. The fact that the predominant Sia species differed between non-activated and activated T cells, and between non-GC T_{FH} cells and GC T_{FH} cells, prompted us to explore the biological functions of the two Sia species in terms of T-cell activity.

Sialoglycans vary greatly in structure and participate in various intermolecular and intercellular interactions via recognition by lectins, including selectins and sialic acid-binding immunoglobulin-like lectins (siglecs), which are expressed principally by immune cells (26). Most siglecs are thought to negatively modulate cellular signaling via the actions of immunoreceptor tyrosine-based inhibitory motifs located in their cytosolic regions, but sialoadhesin (Sn, Siglec-1, CD169) has a short cytosolic region and extended extracellular domains, and it plays a role in cell-cell interactions (27, 28).

In the present study, we found that Neu5Gc-containing glycans negatively regulated T-cell proliferation. Activated T cells escaped from this Neu5Gc-mediated suppression by repression of CMAH. Activation-dependent Neu5Gc suppression was detected by cellular siglecs. Neu5Gc suppression upon T-cell activation was associated with increases in the expression of Sn and Siglec-F ligands, with concomitant loss of the CD22 ligand. The loss of the CD22 ligand reduced the extent of antigen-independent T cell-B cell interactions mediated by CD22. Here we reveal the biological significance of physiological activation-dependent dynamic changes in T-cell sialoglycan expression, in the context of the target cells with which lymphocytes interact. Collectively, our results suggest that suppression of Neu5Gc expression in activated T cells plays a physiologically significant role in immune regulation, involving both T cell-autonomous and heterocellular interaction-mediated mechanisms.

EXPERIMENTAL PROCEDURES

Mice—C57BL/6J, *Cmah* knock-out (*Cmah*$^{-/-}$) (4), and *Cd22* knock-out (*Cd22*$^{-/-}$) (29) mice were housed in a specific-pathogen-free facility. *Cmah* transgenic (Tg) mice were generated via microinjection of a transgenic construct featuring FLAG-tagged mouse *Cmah* cDNA (30) with the mouse *E*μ enhancer, a mouse Ig heavy-chain promoter, and a rabbit β-globin polyadenylation signal. A purified NotI fragment containing the transgene was injected into fertilized eggs of the mouse 129 strain. Tg mice were back-crossed at least five times with C57BL/6J animals prior to analysis. All animal work was performed in accordance with animal care guidelines and was approved by the Animal Experimental Committee of Kyoto University Graduate School of Biostudies.

Materials—Most materials were obtained from Wako Chemical or Nacalai Tesque and met experimental requirements.

Antibodies—The antibodies used were as follows: a phycoerythrin (PE)-conjugated F(ab')$_2$ fragment of anti-rat IgM (Rockland); a PE-conjugated anti-human IgG Fc fragment (Southern Biotech); HRP-conjugated anti-rabbit IgG and HRP-conjugated anti-goat IgG (Zymed Laboratories Inc.); an anti-actin (Santa Cruz Biotechnology, Inc.); FITC- or R-PE-conjugated anti-CD4, R-PE-conjugated anti-CD8 and FITC-conjugated anti-CD69 (BD Biosciences); and PE-conjugated anti-TCR and PE-conjugated anti-CD25 (eBioscience). A rabbit N8 antiserum was used to detect CMAH, as reported previously (31). The supernatant of hybridoma HB-254 cells (from ATCC) cultured in CELLine Flasks (BD Biosciences) was dialyzed against phosphate-buffered saline (PBS) and used as a source of GL7 antibody. The following antibodies were used to stimulate T cells: a purified NA/LE anti-CD28 antibody (BD Biosciences) and an anti-CD3 antibody purified from the culture supernatant of the hybridoma clone 145-2C11 with the aid of Thiophilic superflow resin (Clontech).

Cell Preparation and Culture—Splenocytes were prepared via ACK (ammonium-chloride-potassium) lysis of red blood cells. Splenic T cells were obtained via B220 and CD11b depletion, and B cells were obtained by Thy1 depletion using the MACS system (Miltenyi Biotec). The obtained fractions were stained with an anti-TCR or B220 antibody (BD Biosciences) and analyzed via flow cytometry to confirm T- or B-cell enrichment. T cells were prepared and cultured in RPMI 1640 medium (Invitrogen) supplemented with 10% (v/v) fetal bovine serum (FBS), sodium pyruvate (Invitrogen), nonessential amino acids (Invitrogen), l-glutamine, 2-mercaptoethanol, and kanamycin.

For T-cell activation, anti-CD3 antibodies were immobilized onto cell culture plates or dishes in PBS overnight at 4 °C, and the plates or dishes were washed with culture medium prior to the addition of cells. ConA and anti-CD28 were added to the culture in soluble form.

Preparation of Siglec-Fc Probes—Recombinant mSn-Fc, mCD22-Fc, mCD22(R130A)-Fc, hCD22-Fc, mSiglec-E-Fc, and mSiglec-F-Fc contain the first three domains (the V-set domain and two C2-set domains) of the siglecs and the Fc region of human IgG1. Siglec-Fc probes were produced in sialylation-deficient Lec2 cells and purified with the aid of Protein A-Sepharose, as described previously (4). In mCD22(R130A)-Fc, the arginine residue at position 130 of mouse CD22 (required for ligand binding) was mutated to alanine. Thus, mCD22(R130A)-Fc served as a negative control probe. When flow cytometry was to be performed, the Siglec-Fc probes were precomplexed with PE-conjugated anti-human IgG Fc in FACS buffer (1% (w/v) bovine serum albumin (BSA) and 0.1% (w/v) NaN_3 in PBS) at 4 °C for at least 2 h, and staining then proceeded for 1 h, either at room temperature or on ice.

Flow Cytometry—Staining was performed in FACS buffer. Either FACScan or a FACSCalibur (BD Biosciences) was used, and data were analyzed with the aid of FlowJo software (Tree Star).

High Performance Liquid Chromatography (HPLC) of Sias—Neu5Gc/Neu5Ac ratios were determined using the 1,2-diamino-4,5-methylenedioxybenzene method for detection of α-keto acids, as described previously (31). Briefly, Sias were released by incubating cells in 2 M acetic acid for 2 h at 80 °C. The Sias were then derivatized with 1,2-diamino-4,5-methylenedioxybenzene (Dojindo) and analyzed on a reverse-phase column (TSK-GEL ODS-120T, Tosoh) using a Shimadzu LC10 HPLC system in gradient elution mode.

Western Blotting—After 48 h of stimulation, cells were harvested, washed in PBS, and lysed by sonication in detergent-free lysis buffer (50 mM Tris-HCl (pH 7.6), 1 mM EDTA, Protease Inhibitor Cocktail (Nacalai Tesque)). The supernatant of each ultracentrifuged lysate was collected as the cytosolic fraction and subjected to SDS-PAGE.

5-(and-6)-Carboxyfluorescein Diacetate, Succinimidyl Ester (CFSE) Assay—Splenic T cells were labeled with CFSE by incubating them in labeling buffer (5 μM CFSE and 5% (v/v) FBS in PBS) for 5 min at room temperature with manual cell dispersal every minute. After 48 h of culture, the cells were stained with Siglec-Fc probes and evaluated via FACScan.

Assessment of Proliferation Using an Enzyme-linked Immunosorbent Assay (ELISA)—Aliquots (100 μl) of a splenic T-cell suspension (1×10^6 cells/ml) were placed in the wells of 96-well plates and stimulated with various reagents. After 24 h of culture, bromodeoxyuridine (BrdU) was added, and incubation continued overnight. Incorporated BrdU was detected using a chemiluminescent ELISA system (Roche Applied Science) and a SpectraMaxL (Molecular Devices).

Sialoglycan Expression Modulation of Human Cell Lines—Mouse *Cmah* cDNA was transfected to the U937 cell line with the aid of a retroviral vector that co-expresses green fluorescent protein (GFP) by virtue of the presence of an internal ribosomal entry site (IRES). The KMS-12-PE cell line was stably transfected with rat *St6gal1* cDNA with the aid of a retroviral vector, co-expressing the extracellular domain of human CD4, also by virtue of translation from an IRES. Virus-infected CD4-positive cells were sorted on a FACSAria II cell sorter to obtain cells remodeled in terms of the Sia linkage. Sorted cells were further transfected with mouse *Cmah* cDNA with the aid of a retroviral vector co-expressing GFP by virtue of the presence of an IRES. This construct was used to manipulate Neu5Gc expression. Empty virus vectors served as controls.

Cytotoxic T Lymphocyte (CTL) Assay—CTL activity was measured as reported previously (32), with minor modifications. *Cmah*-Tg or wild-type male mice 8–26 weeks of age were subjected to immunization. Ovalbumin (OVA)-conjugated latex beads (5 μl/mouse; with 168 μg/ml OVA) were suspended in PBS and intravenously injected in combination with *Escherichia coli*-derived lipopolysaccharide (10 ng/mouse). OVA-free latex beads served as controls. One week later, immunized mice were intravenously injected with a 1:1 mixture of OVA-loaded target cells and internal standard (IS) cells. The target/IS cells were prepared from wild-type splenic B cells obtained from ACK-lysed splenocytes using a MACS CD43 depletion system (Miltenyi Biotec). After prewarming for 5 min at 37 °C, B cells were fluorescently labeled with CFSE (2.5 μM for target cells and 0.5 μM for IS cells) for 30 min at 37 °C. Target cells were then further incubated with OVA peptide (OT-I) (1 μM) for 1 h at 37 °C to load the peptide onto the cell surface. Next, target and IS cells were mixed in equal proportions and injected into the immunized mice (1×10^7 target cells and 1×10^7 IS cells). Splenocytes from the recipients were prepared 24 h later, and CFSE-positive cells were counted via flow cytometry. CTL activity was calculated using the following formula.

$$\text{CTL activity (\%)} = \left(1 - \frac{aT}{C}\right) \times 100 \qquad \text{(Eq. 1)}$$

where C represents internal standard cell (%), T is target cell (%), $C_{\text{unimmunized}}$ is C of unimmunized mouse (%), $T_{\text{unimmunized}}$ is T of unimmunized mouse (%), and $a = C_{\text{unimmunized}}/T_{\text{unimmunized}}$ (normalization index). We chose this normalization method because the percentages of target cells (T) were less than those of IS cells (C), even in unimmunized mice. This was probably attributable to CFSE-mediated cytotoxicity and not to variation in CTL activity. Therefore, we used the CTL activity values of unimmunized mice to discriminate responders from non-responders.

Cell-Cell Interaction Assay—Splenic B and T cells of various genetic backgrounds were prepared in 1% (w/v) BSA/PBS rather than RPMI medium with FBS to avoid FBS-mediated contamination with sialylated glycans. B cells were labeled with 5 μM CFSE for 5 min at room temperature, and T cells were labeled with 16 μM FM4-64 (Invitrogen) for 30 min at 37 °C. Labeled B and T cells were washed in 1% (w/v) BSA/PBS, resuspended in the same solution at 2×10^7 cells/ml, and mixed in equal proportions. After incubation for 3 h on ice, samples were diluted in FACS buffer, and fluorescence intensities were measured using a FACSCalibur. The two-celled area was gated on a forward scatter-side scatter plot, and the contributions to fluorescence of CFSE and FM4-64 were analyzed.

Statistical Analysis—Data are expressed as means ± S.E. of the results of (at least) triplicate cultures or of three mice in any group. The statistical significance of observed differences was evaluated using Student's *t* test. All experiments were performed at least twice, and representative results are shown.

RESULTS

Activation-dependent Induction of the Expression of α2,3-linked Neu5Ac in T Cells—Changes in glycosylation patterns modulate protein function, and glycosylation is tightly controlled to optimize the immune response (33). Differences in the Sia species expressed by resting and activated T cells may modulate T-cell functionality. Glycan functions are commonly mediated by the (often sugar linkage-specific) binding of lectins (glycan-recognizing proteins) (34). Thus, the nature of the Sia linkage to glycans is also important in terms of the sialoglycan functions exercised in T cells. α2,6-Linked Sia levels fell upon activation of T cells via suppression of ST6GalI, a sialyltransferase attaching Sias to Gal via an α2,6 linkage (7). Mature T cells expressed fewer α2,6-linked Sias than did B cells but contained large amounts of α2,3-linked Sias (4). Thus, we hypothesized that α2,3-linked Sia levels would increase upon activation of T cells. We first stained activated T cells with a GL7 antibody and a mouse Sn (mSn)-Fc probe to detect α2,6-linked and α2,3-linked Neu5Ac, respectively (4, 35). Regardless of the activating stimulus employed, T cells became GL7-positive, and a combination of anti-CD3 and anti-CD28 most efficiently induced the GL7 epitope. However, the intensity of GL7 staining was low (Fig. 1*A*). In contrast, activated T cells were strongly stained with mSn-Fc (Fig. 1*B*). These results indicate that activation of T cells features (principally) induction of the Sn ligand, α2,3-linked Neu5Ac, at glycan termini.

We previously found that the changes in Sia species of, and concomitant GL7 epitope expression in, activated B cells were caused by repression of Neu5Gc mediated by suppression of CMAH, which is an indispensable enzyme in Neu5Gc biosynthesis. To clarify GL7 epitope induction in activated T cells, the Neu5Gc/Neu5Ac ratio was examined by HPLC, and CMAH expression levels were measured by Western blotting. This was important, because antibody staining of glycans may mirror Neu5Gc expression using certain types of linkage, and a previous report found that *Cmah* mRNA levels declined in activated T cells, but examination at the protein level was not performed in that study (22). The ratio Neu5Gc/(Neu5Ac + Neu5Gc) fell upon activation, and the extent of such change was negatively correlated with the mSn-Fc staining intensity (Fig. 1, *B* and *C*). CMAH was suppressed in activated T cells, most significantly in anti-CD3 and anti-CD28-stimulated T cells (Fig. 1*D*). Thus, T cells repressed Neu5Gc expression by suppressing CMAH, similar to what is seen in B cells.

Role of CMAH Suppression in Activation-dependent Sn Ligand (α2,3-Linked Neu5Ac) Induction—To confirm that suppression of *Cmah* transcription was responsible for the observed changes in sialoglycan expression patterns, the expression levels of Sn ligands in T cells of *Cmah* Tg mice were determined. Such mice were expected to exhibit Tg-derived *Cmah* expression in B cells (Fig. 2*A*). However, the Tg mice also exhibited leaky expression of Tg-derived *Cmah* in T cells (Fig. 2*B*). Development of both T and B cells in *Cmah* Tg mice appeared to be normal (Fig. 2*C*) (data not shown), and the TCR expression level was comparable with that of wild-type animals (Fig. 2*D*). Therefore, we used Tg T cells to explore the role played by CMAH suppression in terms of Sn ligand induction. When splenic T cells from *Cmah* Tg mice were stimulated with anti-CD3 and anti-CD28 *in vitro*, induction of the Sn ligand was repressed principally via Tg-derived CMAH (Fig. 2*E*). Similarly, the GL7 reactivity of LPS-stimulated Tg B cells was largely suppressed (data not shown). This confirmed that transcriptional *Cmah* repression in activated T cells increased α2,3-linked Neu5Ac levels. It has been reported that T-cell activation may change the levels of various glycans. To determine whether activated T cells exhibited alterations in cell surface glycosylation patterns apart from changes in Sia species, we examined activation-dependent cell surface glycan changes on wild-type and *Cmah* Tg T cells by staining with various lectins, the binding of which is associated with sialylation. As expected, the PNA epitope was induced upon activation on both wild-type and *Cmah* Tg T cells (Fig. 2*F*). PNA epitope induction was accompanied by induction of the SNA and MALII epitopes, binding to α2,6 and α2,3 sialoglycans, respectively, independent of Sia modification. Thus, T-cell activation triggered induction of various sialoglycans, whereas *Cmah* Tg T cells exhibited a reduction in only Sn ligand expression, of all lectins tested (Fig. 2*F*).

A Hyperresponsive Phenotype of Neu5Gc-null T Cells—To determine the T cell-autonomous role played by Neu5Gc, we first analyzed the T-cell phenotype of *Cmah* knock-out ($Cmah^{-/-}$) mice, which lack Neu5Gc and thus are useful in exploration of Neu5Gc functions during T-cell activation. Neu5Gc-null $Cmah^{-/-}$ mice exhibited normal T-cell development, as judged by expression of cell surface antigens (Fig. 3, *A–C*). Although T cells developed and matured normally, Neu5Gc-null T cells exhibited a hyperresponsive phenotype after stimulation with ConA or with anti-CD3 and anti-CD28. The proportion of $Cmah^{-/-}$ T cells expressing activation markers (CD25 and CD69) was higher than in wild-type T cells (Fig. 4*A*). This was attributable to hyperactivation because the TCR expression level of, and the extent of ConA binding to, $Cmah^{-/-}$ T cells were comparable with those in wild-type T cells (Figs. 3*B* and 4*B*). Thus, the results suggest that $Cmah^{-/-}$ T cells were hyperreactive to stimulation.

Lack of Neu5Gc in B cells augmented B-cell proliferation (4). Expression of an activation marker may be distinct from T-cell

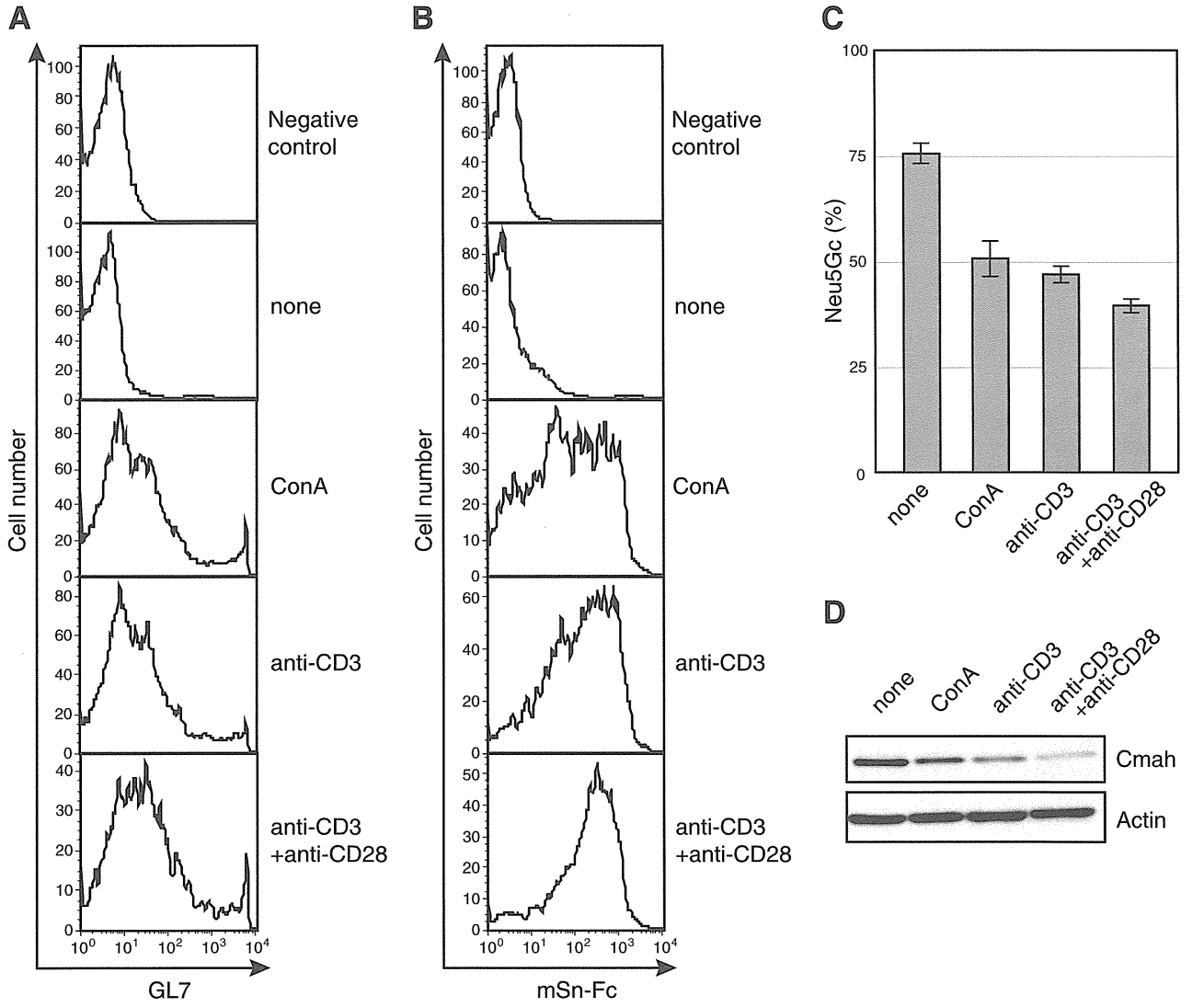

FIGURE 1. **Activation-dependent suppression of Neu5Gc biosynthesis by T cells.** *A* and *B*, splenic T cells were stimulated with ConA (5 μg/ml) or anti-CD3 antibody (5 μg/ml) with or without anti-CD28 antibody (0.5 μg/ml). After 48 h, the cells were stained with GL7 (*A*) or mSn-Fc (*B*) and analyzed by flow cytometry. Propidium iodide-negative (live) cells were analyzed in terms of expression of the GL7 epitope or Sn ligand. *Negative control*, negative controls for staining. *None*, unstimulated samples. Data are representative of the results of more than four independent experiments that yielded similar results. *C*, splenic T cells were stimulated as in *A* above for 48 h and hydrolyzed with acetic acid to release Sias from glycans. The Sias were derivatized using 1,2-diamino-4,5-methylenedioxybenzene, and the ratio of Neu5Gc to total Sias (Neu5Ac + Neu5Gc) was measured using reverse-phase HPLC. *None*, unstimulated samples. Data are means of 3–5 independent experiments. *Error bars*, S.E. *D*, splenic T cells were stimulated as in *A* for 48 h and lysed in detergent-free lysis buffer. The supernatant after ultracentrifugation (the cytosolic fraction) was subjected to Western blotting. *None*, unstimulated samples. Data are representative of three independent experiments that yielded similar results.

proliferation (36). Therefore, we explored whether an increase in the proportion of activated T cells was caused by enhanced proliferation of such cells. We measured proliferation by assessing bromodeoxyuridine incorporation. Compared with wild-type T cells, *Cmah*$^{-/-}$ T cells exhibited enhanced proliferation after being subjected to various types of stimulation (Fig. 4*C*). This indicated that Neu5Gc-containing glycans negatively regulated T-cell proliferation, although the precise mechanism remains unclear. In contrast, *Cmah* Tg T cells proliferated to an extent that was almost the same as that of the wild-type control, at least in terms of immediate early proliferation (data not shown). This is understandable; both wild-type and *Cmah* Tg T cells express Neu5Gc abundantly when stimulated.

Activation-dependent Changes in Siglec Ligand Expression on T Cells—Sias are located in the outermost regions of the cell membrane and play important roles in various molecular recognition events among cells. Thus, changes in Sias can modulate cell-cell interactions. Siglecs distinguish Neu5Gc from Neu5Ac and are expressed principally by immune cells to regulate cell activation. Siglecs have not been identified on mouse T cells, although Siglec-F might be induced in some T-cell populations upon activation (37). Nevertheless, changes in the expression of siglec ligands upon T-cell activation may control immune responses by regulating T-cell recognition by other cell types. To explore the physiological significance of activation-dependent Neu5Gc suppression in T cells further, we examined the expression of siglec ligands by using Siglec-Fc

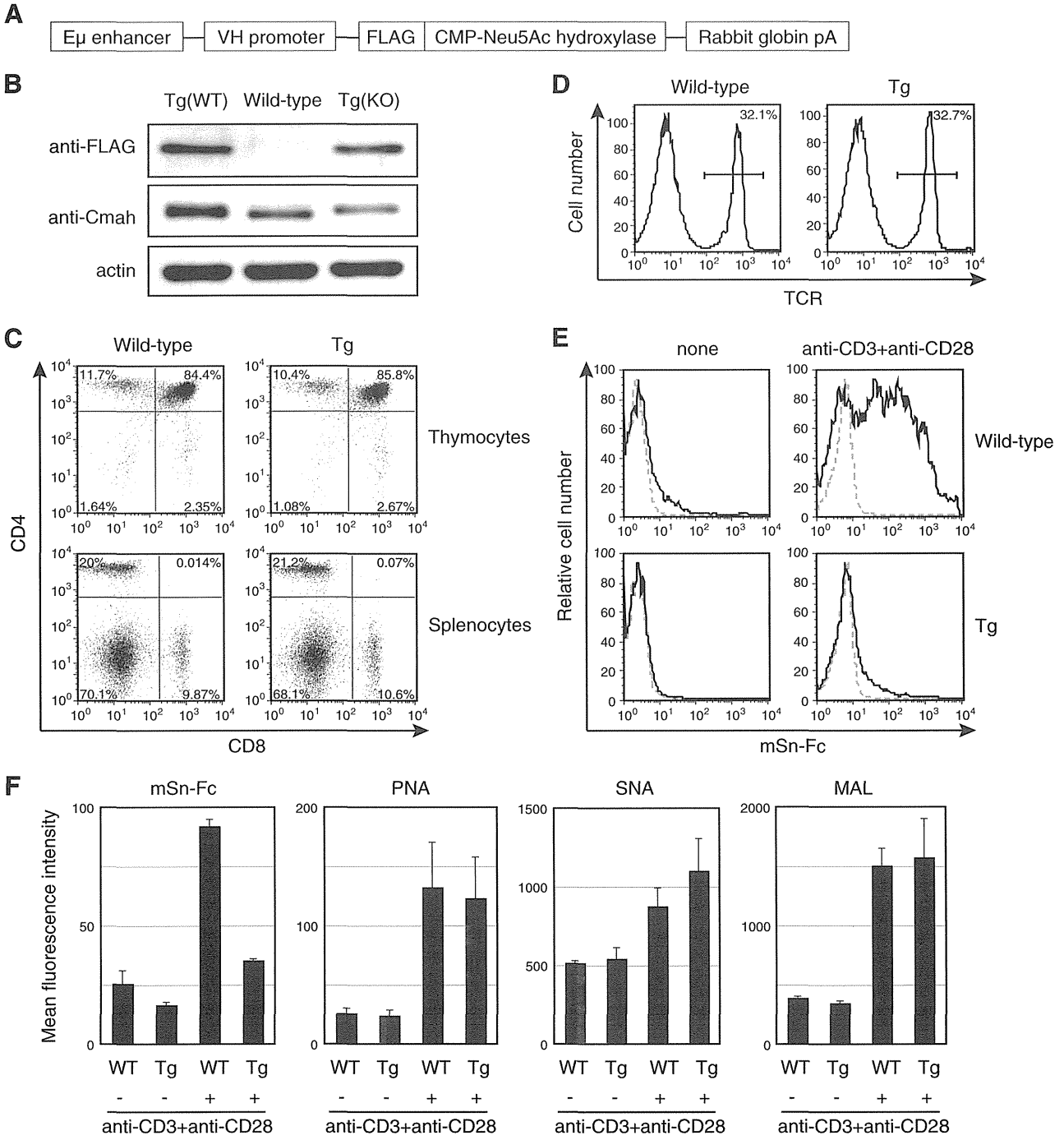

FIGURE 2. **Lack of induction of Sn ligand expression in T cells from *Cmah* Tg mice.** *A*, a schematic of *Cmah* transgene construction. *B*, expression of transgene-derived CMAH in splenic T cells was examined by Western blotting using an anti-FLAG antibody, and total CMAH levels were quantitated using an anti-CMAH N8 antibody. *Tg(WT)* and *Tg(KO)*, transgenic mice of the wild-type and *Cmah*$^{-/-}$ backgrounds, respectively. *C*, thymocytes and splenocytes from wild-type and *Cmah* Tg mice were co-stained with anti-CD4 and anti-CD8 antibodies. Data are representative of three independent experiments that yielded similar results. *D*, splenocytes from wild-type and *Cmah* Tg mice were stained with anti-TCR antibody, and the percentages of TCR-positive T cells are shown. Data are representative of three independent experiments that yielded similar results. *E*, splenic T cells from wild-type and *Cmah* Tg mice were stimulated with anti-CD3 (5 μg/ml) and anti-CD28 (0.5 μg/ml) antibodies for 48 h and stained with mSn-Fc. *None*, unstimulated samples. *Black solid lines*, results obtained upon staining for mSn-Fc; *gray dashed lines*, results of control staining with mCD22(R130A)-Fc. Data are representative of more than two independent experiments that yielded similar results. *F*, splenic T cells from wild-type and *Cmah* Tg mice were stimulated with anti-CD3 (5 μg/ml) and anti-CD28 (0.5 μg/ml) antibodies for 48 h, and cell surface glycan expression was probed using mSn-Fc or the plant lectins PNA (which binds to desialylated core 1), SNA (which binds to α2,6 Sia), and MALII (which binds to α2,3 Sia). The blastic population was gated for the analysis of the fluorescence intensities of activated T cells to ensure that staining intensities were not affected by the numbers of activated cells. Data are the means of three mice per genotype. *Error bars*, S.E.

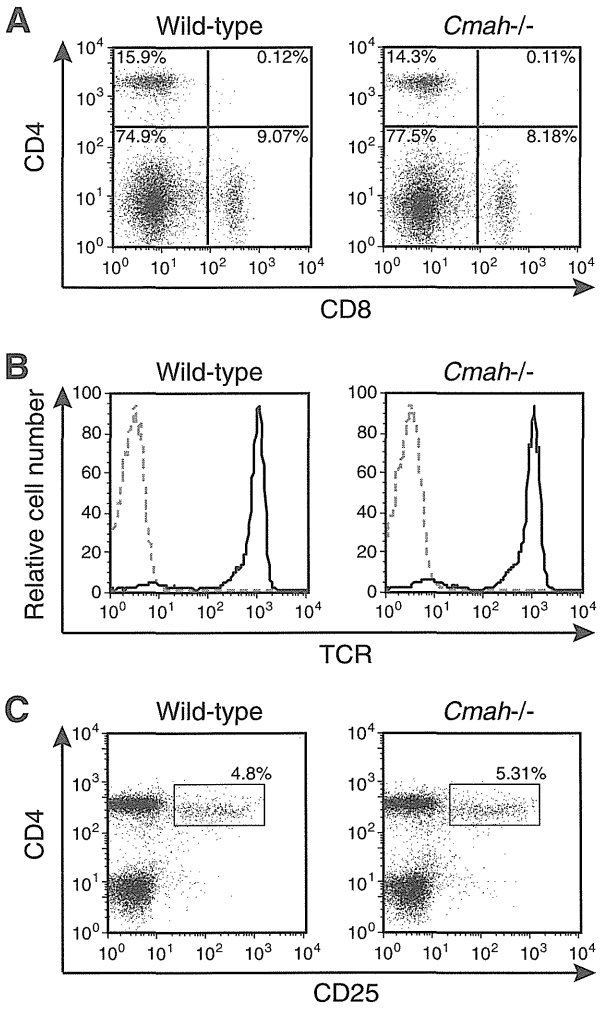

FIGURE 3. **Normal T-cell development in *Cmah*$^{-/-}$ mice.** *A*, splenocytes of wild-type and *Cmah*$^{-/-}$ mice were co-stained with anti-CD4 and anti-CD8 antibodies and analyzed by flow cytometry. *B*, splenic T cells of wild-type and *Cmah*$^{-/-}$ mice were stained with anti-TCR antibody and analyzed by flow cytometry. *Black solid lines*, results obtained when anti-TCR antibody was used; *gray dashed lines*, results from unstained controls. *C*, splenic T cells of wild-type and *Cmah*$^{-/-}$ mice were co-stained with anti-CD4 and anti-CD25 antibodies. The percentages of CD4$^+$CD25$^+$ regulatory T cells are indicated. Data are representative of several independent experiments that yielded similar results.

probes that bind to specific ligands. Levels of Siglec-F ligands increased upon activation, as was also true of Sn ligands (Fig. 5, *A* and *B*). Siglec-F binds to α2,3-linked Sia and may prefer Neu5Ac to Neu5Gc (38), although preference data are limited. CD22 prefers α2,6-linked Neu5Gc (35). In contrast to Siglec-F, CD22 ligand levels were drastically reduced upon activation (Fig. 5, *A* and *B*). Sn, CD22, and Siglec-F are expressed on macrophages, B cells, and eosinophils, respectively. Activation-dependent dynamic changes in the expression levels of siglec ligands may regulate the interaction of T cells with such cells.

When activated T cells were stained with the mSn-Fc probe, the binding strength varied (Figs. 1*B* and 5*B*). Apart from the observed reduction in Neu5Gc biosynthesis after CMAH repression, cellular division may contribute to the observed decrease in Neu5Gc-containing glycan levels by diluting the Neu5Gc cytosolic pool. To explore a possible association between changes in siglec ligand levels and division of T cells, CFSE-labeled splenic T cells were activated with anti-CD3 and anti-CD28 and then stained with GL7 (detecting α2,6-linked Neu5Ac), mSn-Fc (α2,3-linked Neu5Ac), mCD22-Fc (α2,6-linked Neu5Gc), and hCD22-Fc (α2,6-linked Neu5Ac and Neu5Gc). Cells that had undergone more division cycles expressed higher levels of Sn ligands (Fig. 5*C*). Such cells expressed the GL7 epitope. However, only a proportion of the activated T cells were GL7-positive (Figs. 1*A* and 5*C*). The partial (and mild) increase in GL7 epitope expression and the marked decrease in CD22 ligand levels may have been caused by a fall in α2,6-linked Sia levels on activated T cells. This suggestion is supported by the results of staining with hCD22-Fc and by DNA microarray transcriptome data from anti-CD3-plus-IL-2-stimulated T cells (7). The observed mild increase in SNA staining (Fig. 2*F*) (SNA also binds to α2,6-sialoglycans) may reflect augmentation of cellular surface area, because the blastic population was gated to retain only activated cells in Fig. 2*F*. Such gating was applied to eliminate any influence of differences in the proportions of activated cells among genotypes.

Recently, the Siglec-E ligand (but not the Sn ligand) was reported to be induced upon activation of T cells (22). However, we found that, under our experimental conditions, the mSiglec-E-Fc probe did not bind to mouse T cells, regardless of whether such cells were stimulated (Fig. 5, *D* and *E*). In line with this result, *Cmah*$^{-/-}$ T cells lacking Neu5Gc did not express the Siglec-E ligand, regardless of activation status (Fig. 5, *D* and *E*). In contrast, *Cmah*$^{-/-}$ T cells were stained strongly with mSn-Fc, independent of activation status. To confirm further that the Siglec-E ligand was not induced by the change in Sia species mediated by regulation of CMAH expression, *Cmah* cDNA was transfected into "mSiglec-E-Fc-positive" U937 cells, and the effect on mSiglec-E-Fc staining was examined. U937 cells, a human monocytic cell line, lack CMAH and thus express Neu5Ac exclusively. If Siglec-E strongly prefers to bind to Neu5Ac rather than Neu5Gc, as indicated, expression of exogenous CMAH would reduce the intensity of mSiglec-E-Fc staining. However, mSiglec-E-Fc staining was not affected by *Cmah* transfection, whereas α2,3-linked Neu5Ac-detecting mSn-Fc staining decreased in proportion to the increase in CMAH expression (as monitored by the synthesis of GFP) (Fig. 6, *A–C*). A human myeloma cell line, KMS-12-PE, was also used to examine the effect of CMAH induction on Siglec-E ligand expression. *Cmah* transfection into KMS-12-PE cells slightly reduced staining by mSiglec-E-Fc, but mSn-Fc and mSiglec-F-Fc staining was greatly reduced (Fig. 6*D*) (data not shown). From these results, we concluded that our Siglec-Fc probes functioned appropriately. Together, the data suggest that Siglec-E may prefer to bind to Neu5Ac-containing glycans rather than Neu5Gc-containing glycans, at least on human myeloma KMS-12-PE cells, as previously reported (22), although the preference was much lower than those exhibited by Sn or Siglec-F.

When activated *Cmah*$^{-/-}$ T cells were stained with mSn-Fc, two peaks were observed (Fig. 5*D*). Therefore, apart from Sia species, Sn can preferentially recognize certain T-cell populations. To determine the T-cell subpopulations that exhibited higher level expression of Sn ligands, wild-type and *Cmah*$^{-/-}$ T

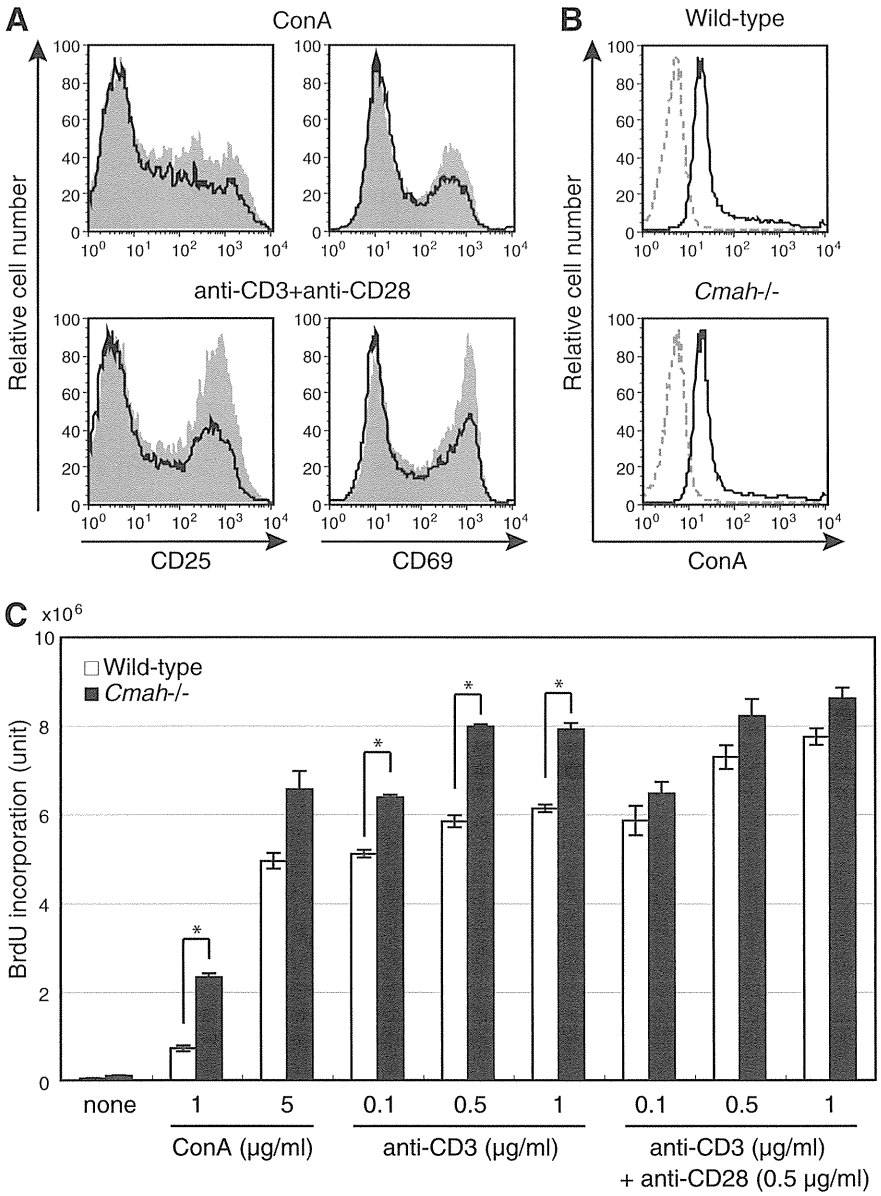

FIGURE 4. **The hyperresponsive phenotype of Neu5Gc-null T cells.** *A*, splenic T cells from wild-type (*black/line*) and *Cmah*$^{-/-}$ (*gray/filled*) mice were stimulated with ConA (5 μg/ml) or with anti-CD3 (0.5 μg/ml) and anti-CD28 (0.5 μg/ml) antibodies. After 2 days, cells were stained with anti-CD25 or anti-CD69 antibodies and analyzed by flow cytometry. Data are representative of three independent experiments that yielded similar results. *B*, splenic T cells of wild-type and *Cmah*$^{-/-}$ mice were stained with FITC-conjugated ConA. *Gray dashed lines*, negative control values. Data are representative of three independent experiments that yielded similar results. *C*, splenic T cells of wild-type (*open columns*) and *Cmah*$^{-/-}$ (*filled columns*) mice were stimulated with the indicated concentrations of ConA or of anti-CD3 and anti-CD28 antibodies for 24 h, and BrdU was then added. After overnight incubation, incorporated BrdU was detected by ELISA, and it is expressed in chemiluminescence units. *None*, unstimulated samples. Data are the means of values from triplicate cultures. *Error bars*, S.E. Data are representative of more than three independent experiments that yielded similar results. *, difference between the test and control data was statistically significant by Student's *t* test ($p < 0.01$).

cells were co-stained with anti-CD8 antibody and mSn-Fc. The results show that more Sn ligands were expressed in CD8$^+$ T cells when Neu5Ac was the predominant Sia species present (Fig. 7*A*). After activation, Sn ligand expression was induced in both CD8$^+$ and CD4$^+$ (CD8$^-$) T cells (Fig. 7*B*) of wild-type mice because *Cmah* was suppressed. In contrast, although *Cmah*$^{-/-}$ CD4$^+$ (CD8$^-$) T cells induced such expression, the level of Sn ligands in CD8$^+$ T cells was slightly reduced. Collectively, the data indicate that although CMAH plays a major role in induction of Sn ligand expression in activated T cells, other enzyme(s) can also modulate Sn ligand expression, depending on the T-cell subpopulation in question (Figs. 5 (*D* and *E*) and 7 (*A* and *B*)). Recently, accumulating data suggest that T cells are targets of Sn$^+$ macrophages (39). Thus, depending on the T-cell subpopulation, differences in Sn ligand expression levels may determine the extent and nature of subsequent antigen presentation by macrophages or dendritic cells (DCs) expressing Sn, also termed CD169.

The above results lead us to conclude that activated T cells up-regulate the expression of Sn and Siglec-F ligands but not

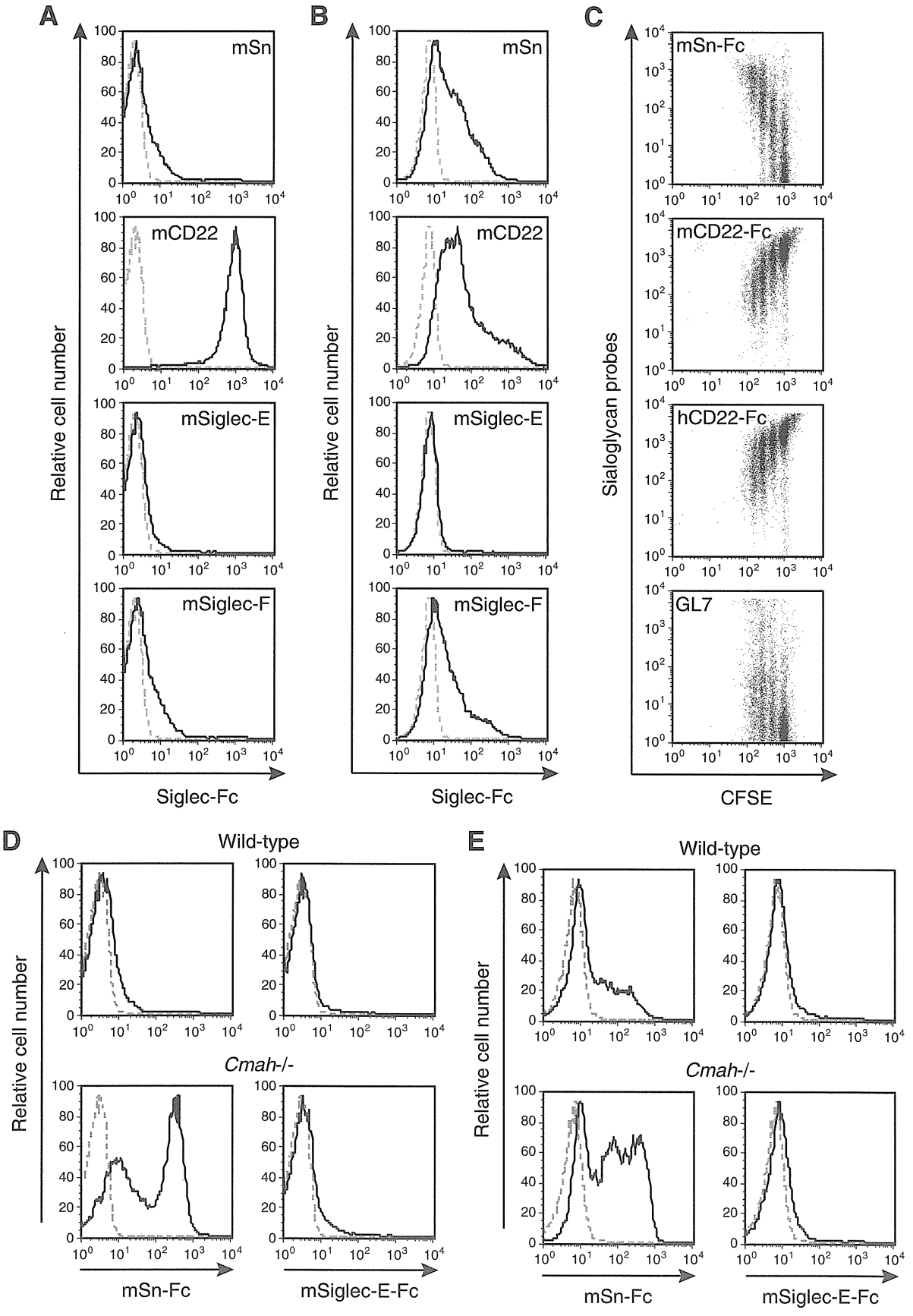

Siglec-E ligands. Concomitantly, activated T cells down-regulate the expression of CD22 ligand. Such dynamic changes in the siglec ligand expression profile may regulate the interaction of T cells with other immune cells expressing siglecs. It is possible that certain siglecs are expressed on particular T-cell subpopulations. In addition, we cannot rule out a possible effect of currently unknown novel siglecs expressed on T cells or other cell types. Very recently, activation-dependent induction of Sn ligand expression by $CD4^+$ effector T cells has been reported. The cited work focused on changes in the Sia linkage rather than the Sia species *per se* and concluded that α2,3-sialyltransferases such as ST3Gal6 may be responsible for induction of Sn ligand expression in such cells (40). Our data suggest that *Cmah* suppression in activated $CD4^+$ effector T cells may also contribute to increased expression of Sn ligands.

Enhanced CTL Activity in CMAH Tg Mice—To evaluate the functional aspects of Sn/CD169 ligand expression by activated $CD8^+$ T cells, we used Sn/$CD169^+$ cells as antigen-presenting cells and measured CTL activity (39, 41) using *Cmah* Tg mice, because *Cmah* Tg T cells suppress activation-dependent Sn/CD169 ligand induction (Fig. 2*E*) but would be expected to be very similar to wild-type T cells prior to activation. Intravenously injected latex particles are phagocytosed in the spleen (principally by Sn/$CD169^+$ cells and $CD11c^+$ DCs). At a later time point, activated DCs present antigen to T cells in the T-cell zone (42). Therefore, after loading OVA-conjugated latex beads to Sn/$CD169^+$ cells *in vivo*, we measured CTL activity directed toward OVA peptide (OT-I)-loaded target cells (32) to determine whether induction of Sn/CD169 ligand expression in activated $CD8^+$ T cells would affect this activity. We immunized mice with OVA-latex beads and LPS as an adjuvant and measured *in vivo* lysis of OVA peptide-loaded target cells (Fig. 7*C*). Some Tg mice (strong responders) exhibited higher levels of cytotoxic activity (>40% lysis), but none of the wild-type mice were strong responders. Other Tg mice responded less strongly, similar to the wild-type controls (Fig. 7*D*). Overall, the difference between the responses of the Tg mice and the controls was not particularly marked and was considered to be attributable to the presence of strong responders among the Tg mice. The precise mechanism of such enhanced CTL activity in *Cmah* Tg mice is unknown, but induction of Sn/CD169 ligand expression seems to play a negative role, suggesting that interaction between activated T cells and Sn/$CD169^+$ cells negatively affects the immune response at later time points (see "Discussion").

Enhanced CD22-mediated T Cell-B Cell Interaction (T-B Interaction) after Suppression of Neu5Gc Expression by B Cells—Activated T cells no longer expressed CD22 ligands upon induction of Sn ligand expression (Fig. 5*C*). We have previously shown that GC B cells exhibit down-regulation of CD22 ligand expression, as detected using a GC marker, GL7 (4). We hypothesized that this might be interpreted as loss of *cis*-ligands, possibly increasing interactions with *trans*-ligands. However, the nature of the cells expressing *trans*-ligands for GC B cells remains unclear. GL7-positive unmasked B cells (lacking CD22 ligands) were located almost exclusively within GCs. Other cells of GCs include T_{FH} cells, which transmit the activation signals required for appropriate B-cell activation in an antigen-dependent manner. GC T_{FH} cells are GL7-positive, as are B-cell populations (23). Fig. 1 shows that T-cell activation repressed Neu5Gc synthesis. Thus, we hypothesized that concomitant Neu5Gc suppression in both T and B cells might control the extent of interactions between these cells. We explored antigen-independent Sia modification-dependent T-B interactions by using an assay employing "untouched" splenic T cells and B cells. This was advantageous, because the binding of antibody to cells may induce various alterations, especially in B cells. To explore the effects of variation in Sia species, we used B and T cells from $Cmah^{-/-}$ mice to model activated B and T cells expressing Neu5Ac as the major Sia species and wild-type B and T cells that express principally Neu5Gc as nonactivated cells. In this model, the full repertoire of TCRs and B-cell receptors (BCRs) were included, and antigen-dependent interactions were thus minimized. We used this *in vitro* T-B interaction assay to explore the veracity of our hypothesis that T cells that fail to suppress Neu5Gc expression may cause Neu5Gc to function as a *trans*-ligand for CD22 (expressed by unmasked B cells), resulting in TCR-independent T-B interaction. When both T and B cells were prepared from wild-type mice, the T-B interaction was minimal (Fig. 8). However, GL7-positive B cells from $Cmah^{-/-}$ mice, which lack *cis*-ligands, exhibited very strong interactions with wild-type T cells, although the BCR/TCR repertoire was similar to that of unbound controls. The extent of this interaction was significant and reproducible under the conditions that we used, although the cell interaction values (percentages) were relatively low (less than 15% of total cells). Neu5Gc is important in this context because the T cells of $Cmah^{-/-}$ mice avoided recognition by unmasked B cells. Because *Cd22* deletion rescued the enhanced T-B interaction phenotype, we concluded that the interaction was mediated by CD22. The data indicated that repression of Neu5Gc in GC B cells increased CD22 binding capacity to *trans*-ligands, thus affecting the binding of such cells to other cells, including T cells. This interaction is thought not to involve TCR (antigen specificity). Activated T cells/GC T_{FH} cells (23) may escape CD22-mediated antigen specificity-independent binding to activated B cells via repression of Neu5Gc-containing glycans (28). Our results thus suggest that a change from Neu5Gc to Neu5Ac production in activated T cells reduces nonspecific

FIGURE 5. **Changes in siglec ligand expression upon activation of T cells.** *A* and *B*, wild-type unstimulated splenic T cells (*A*) or such cells after activation with anti-CD3 (5 μg/ml) and anti-CD28 (0.5 μg/ml) antibodies for 48 h (*B*) were stained using various Siglec-Fc probes and analyzed by flow cytometry. *Black solid lines*, staining data for mSn-Fc, mCD22-Fc, mSiglec-E-Fc, or mSiglec-F-Fc; *gray dashed lines*, results of control staining with mCD22(R130A)-Fc. Data are representative of two independent experiments that yielded similar results. *C*, CFSE-labeled wild-type splenic T cells were stimulated with anti-CD3 (5 μg/ml) and anti-CD28 (0.5 μg/ml) antibodies. After 48 h of culture, the cells were stained with mSn-Fc, mCD22-Fc, hCD22-Fc, or GL7 antibody and analyzed by flow cytometry. Propidium iodide-negative (live) cells were analyzed. Data are representative of more than two independent experiments that yielded similar results. *D* and *E*, wild-type and $Cmah^{-/-}$ splenic T cells without stimulation (*D*) or after activation with anti-CD3 (5 μg/ml) and anti-CD28 (0.5 μg/ml) for 48 h (*E*) were stained with mSn-Fc or mSiglec-E-Fc and analyzed by flow cytometry. The results are shown as in *A*. Data are representative of two or three independent experiments that yielded similar results.

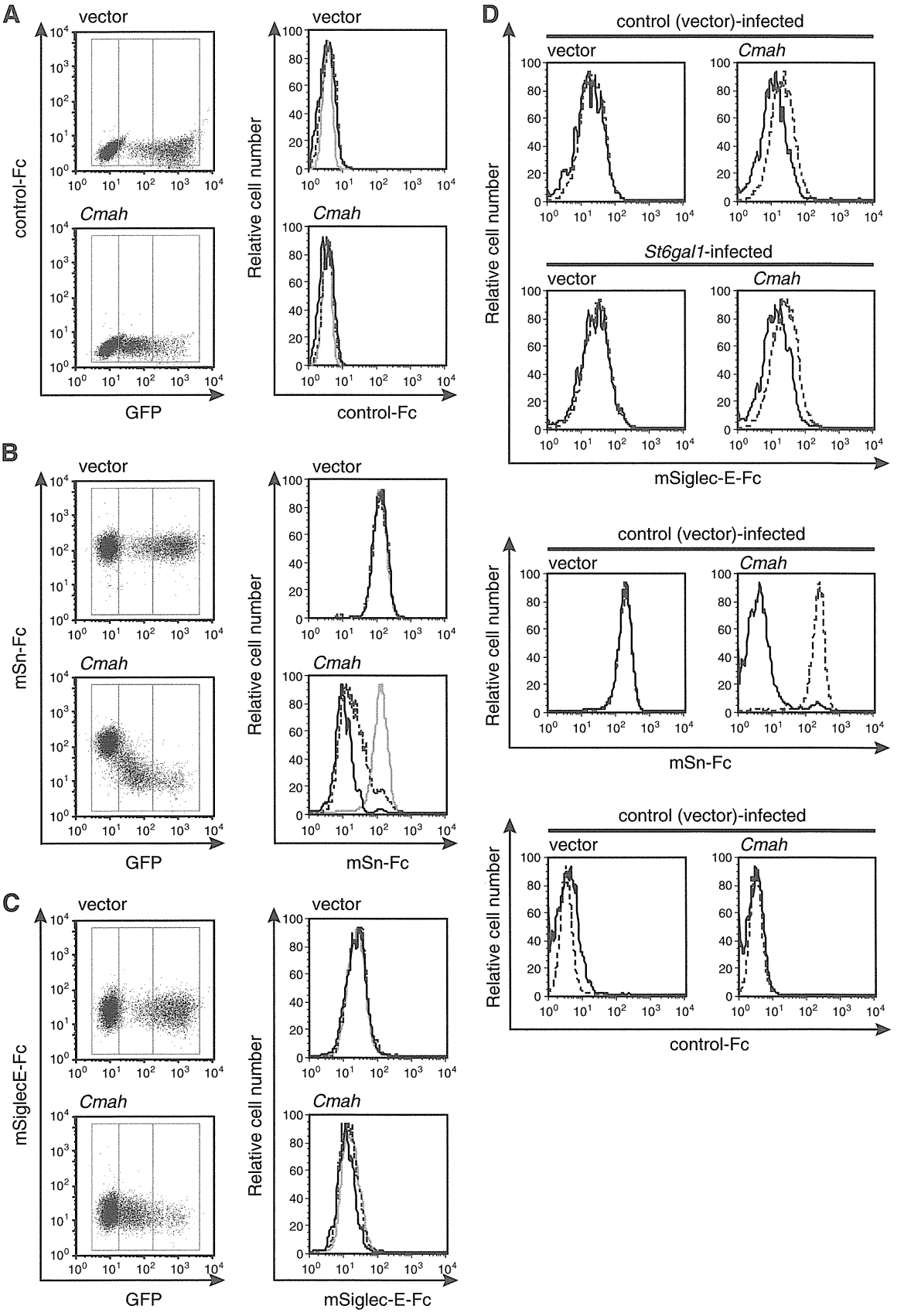

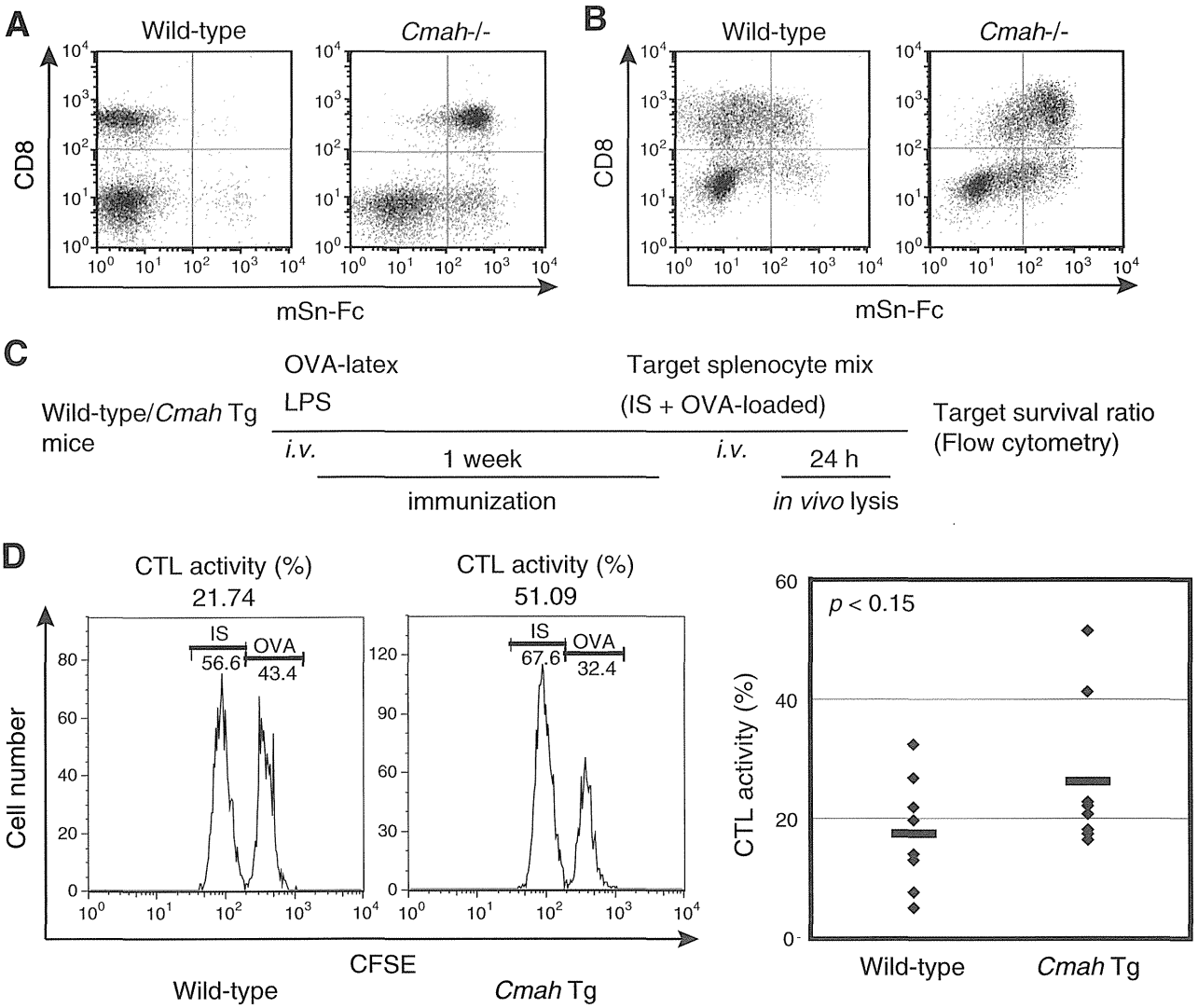

FIGURE 7. **CTL activity in *Cmah* Tg mice.** *A* and *B*, unstimulated fresh wild-type and $Cmah^{-/-}$ splenic T cells (*A*) or such cells after activation with anti-CD3 (5 μg/ml) and anti-CD28 (0.5 μg/ml) antibodies for 48 h (*B*) were co-stained with anti-CD8 antibody and mSn-Fc and analyzed by flow cytometry. Data are representative of two independent experiments that yielded similar results. *C*, the CTL assay. Male wild-type and *Cmah* Tg mice were immunized with OVA-latex particles, and the extent of elimination of OVA peptide-loaded target cells was determined as described under "Experimental Procedures." *D*, CTL activity levels were determined in immunized mice. The histograms on the *left* show representative data used to calculate CTL activity. In the *right panel*, each *diamond* represents the data from an individual mouse, obtained in two independent experiments. *Wide bars*, mean CTL values of each genotype. The statistical significance of observed differences (with respect to the wild-type control) was evaluated using Student's *t* test, and *p* value is shown.

T-B cell interaction and/or prevents CD22-mediated negative signaling in B cells utilizing the *trans*-ligands on T cells.

DISCUSSION

In the present study, we found that Neu5Gc negatively regulated T-cell proliferation, as has also been reported in B cells. We showed that lymphocytes modified their Sias after activation to regulate cellular proliferation (Fig. 4*C*). Very recently, Buchlis *et al.* (43) independently reported enhanced T-cell proliferation in $Cmah^{-/-}$ mice. We examined proliferation at an earlier time point than considered by the cited authors. The cited work examined proliferation of CFSE-labeled cells cultured for 3–5 days. Thus, our results highlight events that take place at a more immediate early TCR-signaling stage. The mechanism by which Neu5Gc regulates T-cell proliferation has yet to be determined; however, the process appears to be CD22-

FIGURE 6. **Changes in siglec ligand expression levels upon expression of CMAH.** *A–C*, *Cmah* cDNA was transfected to U937 cells using a retroviral vector co-expressing GFP from an IRES. The empty vector served as the control. Polyclonal cells expressing CMAH at various levels were stained with the indicated Siglec-Fc probes: mCD22(R130A)-hFc (*A*; negative staining control), mSn-Fc (*B*), or mSiglec-E-Fc (*C*). The *lines* within histograms (on the *right*) indicate gene expression strengths as follows. *Gray solid lines*, GFP-negative cells; *dashed lines*, GFP^{low} cells; *black solid lines*, GFP^{high} cells. *D*, to remodel the Sia linkage, KMS-12-PE cells were retrovirally transfected with *St6gal1* cDNA or the empty vector. Next, virus-infected cells were sorted and further retrovirally transfected with *Cmah* cDNA or the empty vector to manipulate Neu5Gc expression. The retrovirus vector used here co-expressed GFP from an IRES. The cells were stained with the indicated Siglec-Fc probes and analyzed by flow cytometry. *Black solid lines*, results for GFP-positive retrovirus-infected cells; *gray dashed lines*, results for GFP-negative cells. Data are representative of two independent experiments that yielded similar results.

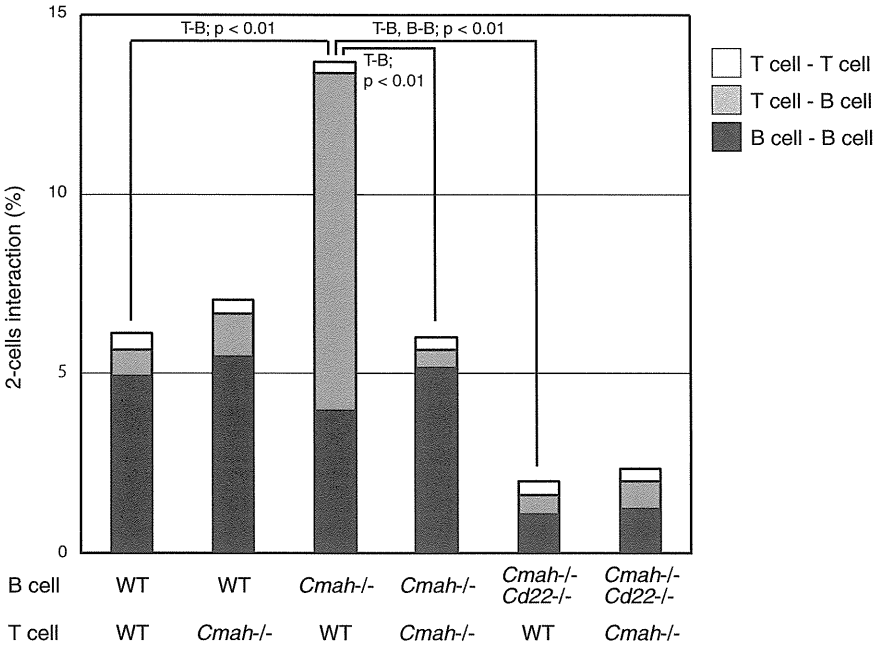

FIGURE 8. **CD22-dependent T cell-B cell interaction between Sia species-remodeled lymphocytes.** Splenic B and T cells prelabeled with CFSE and FM4-64, respectively, were co-incubated in various combinations for 3 h on ice and analyzed by flow cytometry. The two-cell population was gated in the forward scatter-side scatter plot, and the fluorescence intensities of CFSE and FM4-64 were analyzed using a two-color plot, whereby autonomous binding resulted in doubled fluorescence intensity, and heterologous binding resulted in two-color positivity. The calculated percentages of two-cell interactions are graphically indicated. *White*, T cell-T cell; *gray*, T cell-B cell; *black*, B cell-B cell. Genotypes are indicated as wild type (*WT*), *Cmah* knock-out (*Cmah*$^{-/-}$), or *Cmah/Cd22* double knock-out (*Cmah*$^{-/-}$*Cd22*$^{-/-}$). Data are shown as the means of 3–4 independent experiments. The statistical significance of the observed differences between the following combinations was confirmed using Student's *t* test ($p < 0.01$): the T cell-B cell interaction between (wild-type or *Cmah*$^{-/-}$) B cells and wild-type T cells, *Cmah*$^{-/-}$ B cells and (wild-type or *Cmah*$^{-/-}$) T cells, and (*Cmah*$^{-/-}$ or *Cmah*$^{-/-}$*Cd22*$^{-/-}$) B cells and wild-type T cells, and the B cell-B cell interaction between (*Cmah*$^{-/-}$ or *Cmah*$^{-/-}$*Cd22*$^{-/-}$) B cells and wild-type T cells.

independent, because both T and B cells exhibited similar phenotypes, and only B cells express CD22. Although human T cells express low levels of CD33 (Siglec-3)-related siglecs (44), no report has described the siglecs of mouse T cells, with the exception of Siglec-F. This siglec was reportedly not expressed on resting T cells but was induced in some CD4$^+$ T cells in an allergic inflammation model (37). Currently, the role played by Siglec-F in T cells remains unknown, although we did observe Siglec-F ligand induction in activated T cells in which the ligand may function as a *cis*-ligand (Fig. 5*B*). It has been reported that the proliferative response of GL7-stained subpopulations of thymus CD4$^+$CD8$^-$ cells was greater than that of their GL7-unstained counterparts (45). Therefore, expression of the GL7 epitope on thymocytes may also be affected by repression of Neu5Gc, similar to what is seen in activated splenic T cells, enhancing cell proliferation (Fig. 4*C*). Identification of the molecule(s) involved in Neu5Gc-mediated negative regulation of cell proliferation is important because such data might explain the observed differences between humans, who are unable to biosynthesize Neu5Gc, and other hominid species (46).

Recently, the Siglec-E ligand was reported to be up-regulated in activated T cells. Probes for other siglec ligands, including Sn and Siglec-F, bound poorly to activated T cells in the cited report (22). However, we could not detect significant binding of mSiglec-E-Fc to mouse T cells (Fig. 5, *D* and *E*) in our present study. The probe did bind to U937 cells, indicating that the probe was active. The discrepancies in mSiglec-E-Fc binding patterns may be attributable to differences in Fc probe preparation. To prevent potential masking of binding caused by probe sialylation, we used Lec2 cells for probe preparation. These cells do not express Sia on their surface because the Golgi apparatus does not contain a CMP-Sia transporter (47). The utility of this approach should be emphasized, especially for the CD33 subfamily of siglecs, which bind weakly to their ligands, or probes targeting α2,3-linked Sia (the dominant form of sialylation in many cell types, including CHO cells). However, it is also possible that differences in culture conditions may have caused glycan expression levels to vary.

Changes in Sia expression not only regulated lymphocyte proliferation but also modulated cell-cell interactions (Fig. 8). Avoidance of nonspecific T-B interactions in GCs is very important because GC T_{FH} cells form a specialized subset of effector cells that act on GC B cells via cytokine release or co-receptor ligation. It is reasonable to expect that a large proportion of GC B cells do not possess the appropriate BCR because of the random nature of somatic hypermutation that occurs after activation by GC T_{FH} cells. Regardless of BCR status, such cells express unmasked CD22 without alteration of CD22 expression levels, as shown by high level GL7 epitope expression by GC B cells (4). Such GL7-positive (CD22-unmasked) B cells proliferate in GCs, where GC T_{FH} cells also reside. We hypothesized that concomitant Neu5Gc suppression in both activated T (Fig. 1) and B cells (4) might be crucial for regulation of T-B interaction. To evaluate this hypothesis, we established a model system using nonactivated cells to examine the cellular interaction of T cells and B cells in an antigen-nonspecific manner (Fig. 8), because GC cells are blastic and tend to engage in cellular adhesion. Furthermore, GC T_{FH}/B cells cannot be iso-